RESEARCH ARTICLE

Investigation of reactive gases and methane variability in the coastal boundary layer of the central Mediterranean basin

Paolo Cristofanelli*, Maurizio Busetto*, Francescopiero Calzolari*, Ivano Ammoscato†, Daniel Gullì†, Adelaide Dinoi‡, Claudia Roberta Calidonna†, Daniele Contini‡, Damiano Sferlazzo§, Tatiana Di Iorio‖, Salvatore Piacentino¶, Angela Marinoni*, Michela Maione** and Paolo Bonasoni*

We present a characterization of reactive gases (RG: O_3, NO, NO_2, SO_2, CO) and methane (CH_4) variability in the central Mediterranean basin, analyzing in situ measurements at three new permanent WMO/GAW Observatories in Southern Italy: Capo Granitola – CGR (Sicily), Lamezia Terme – LMT (Calabria) and Lecce – ECO (Apulia). At all the measurement sites, a combination of the breeze wind system (especially at CGR and LMT), PBL dynamics, anthropogenic/natural emissions, and photochemistry lead the appearance of well-defined diurnal cycles for the observed RG.

According to O_3/NO_x variability, local emissions appeared to influence CGR and LMT (no NO_x data were available for ECO during the period of study) in 4% and 20% of the hourly data, nearby sources in 39% and 40%, remote sources in 31% and 14%, while background O_3/NO_x were observed in 26% of cases for both the stations. Most of the background O_3/NO_x were observed during daytime, when offshore air masses usually affected the measurement sites. Local sources of CH_4 at CGR can be related to biogenic (oxic) emissions from biomasses along the coastline, while emissions from live stocks can represent a local source of CH_4 at LMT.

Finally, we provide first hints about the export of O_3 from Sicily/Southern Italy to the Mediterranean Sea by comparing simultaneous observations at CGR and Lampedusa (LMP), a small island in the middle of the Strait of Sicily where a WMO/GAW Regional Station is located. In summer, O_3 increased by some 7 ppb for transport times lower than 48 h, while no statistical significant differences were observed for travel time longer than 48. This would suggest that photochemical O_3 production occurred within air-mass travelling from CGR to LMP, but also that the central Mediterranean MBL represents a O_3 sink for relatively aged air-masses.

Keywords: mediterranean basin; reactive gases; methane

Publisher's Note

This article's Funding Information section has been updated to reflect post-publication changes in the funding of this article's publication and open-access costs.

1. Introduction and motivation

Southern Europe and the Mediterranean basin are recognized as hotspot regions both in terms of climate change (e.g. Giorgi and Lionello, 2008) and air quality (Monks et al., 2009), also representing a major crossroads of different

* Institute of Atmospheric Sciences and Climate, National Research Council of Italy, Bologna, IT

† Institute of Atmospheric Sciences and Climate, National Research Council of Italy, Lamezia Terme, IT

‡ Institute of Atmospheric Sciences and Climate, National Research Council of Italy, Lecce, IT

§ ENEA, Laboratory for Observations and Analyses of Earth and Climate, Lampedusa, IT

‖ ENEA, Laboratory for Observations and Analyses of Earth and Climate, Rome, IT

¶ ENEA, Laboratory for Observations and Analyses of Earth and Climate, Palermo, IT

** University of Urbino, Department of Pure and Applied Sciences (DiSPeA), Urbino, IT

Corresponding author: Paolo Cristofanelli (p.cristofanelli@isac.cnr.it)

air mass transport processes (Lelieveld et al., 2002; Henne et al., 2004; Duncan et al., 2008). Meteorological conditions such as frequent clear sky and high solar radiation in summer enhance the formation of photochemical ozone (O_3) due to the availability of natural and anthropogenic precursors. In particular, large amounts of anthropogenic pollutants emitted in continental Europe are transported towards the basin (e.g. Duncan et al., 2008; Henne et al., 2004; Safieddine et al., 2014) where intense photochemical O_3 production occurs (Vautard et al., 2005). Modeling scenarios and satellite investigations show the central Mediterranean basin (i.e. from 5°E to 20°E, see also **Figure 1**) as the region where O_3 is maximized in summer at the surface (Safiedinne et al., 2014). Ricaud et al. (2014) have shown that the meteorology in the Mediterranean basin favors a western basin enriched for instance in methane (CH_4) compared to the eastern basin. Saharan dust outbreaks from Northern Africa (Querol et al., 2009) and widespread open biomass burning (Turquety et al. 2014) further exacerbate air quality and the impact of anthropogenic emissions on the regional climate (Mallet et al., 2013). Even though anthropogenic sulphur dioxide (SO_2) emissions have been significantly reduced, in Europe, offshore traffic ship emissions still represent a significant source of atmospheric SO_2, especially in the central Mediterranean basin (Becagli et al., 2012; EEA, 2013; Cesari et al., 2014; Jalkanen et al., 2016) and the Sicily Strait is characterized by heavy ship traffic, making the central Mediterranean basin a European hotspot for the impact of ship emissions on air chemistry (EEA, 2013). In addition, there are significant interactions with natural emissions, which contribute up to 20% of the total oxidized sulfur production on a mean yearly basis (Kouvarakis and Mihalopoulos, 2002). Water scarcity, the concentration of economic activities in coastal areas, and reliance on climate-sensitive agriculture are other factors that identify this region as one of the most responsive to air pollution and climate change. In addition, the Mediterranean region is undergoing intensive demographic, social, cultural, economic and environmental changes.

Unfortunately, very few atmospheric research observatories in the central Mediterranean basin provided continuous high quality information on atmospheric composition and reactive gases (RG). Until the year 2014, besides the GAW/WMO Mt. Cimone Global Station (located in Northern Italy), only one other regional GAW/WMO station (El Gozo, Malta, see Saliba et al., 2008) provided long-term information on O_3 variability in this region. Only recently (2014, July), continuous O_3 observations have been started at the regional GAW/WMO station "N. Sarao" at Lampedusa Island (central Mediterranean Sea). To increase the amount and quality of environmental information available in the central Mediterranean basin, the Italian Government and the European Union fostered the "I-AMICA"(Infrastructure of High Technology for Integrated Climate and Environmental Monitoring, www.i-amica.it) Project devoted to strengthening (i) an integrated atmospheric-marine-coastal-agro-forestry Observing Systems, (ii) parallel computing infrastructures, (iii) air quality services in the Italian "convergence Region" (i.e. the regions with delayed development, whose per capita gross domestic product is below 75% of the European average). Therefore, the Institute of Atmospheric Science and Climate of the Italian National Research Council of Italy (ISAC-CNR) has built and activated three new Atmospheric Observatories (**Figure 1**) at Capo Granitola (Sicily), Lamezia Terme (Calabria) and Lecce (Apulia).

This work analyses the first full year (January – December 2015) of RG measurements – O_3, nitrogen oxides (NO and NO_2), carbon monoxide (CO), SO_2 and CH_4

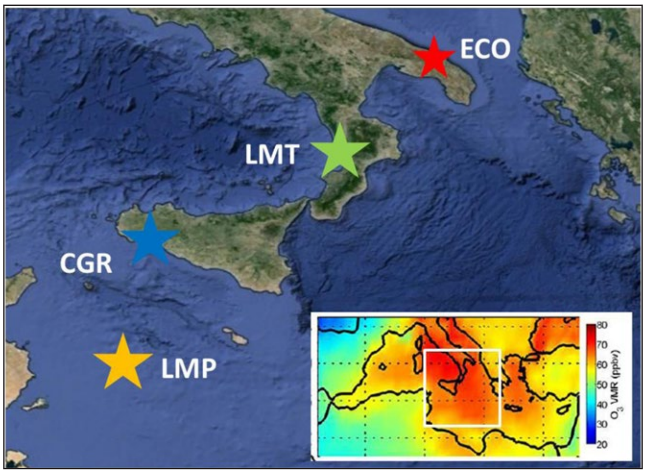

Figure 1: Geographical location of the I-AMICA observatories: Capo Granitola (CGR), Lamezia Terme (LMT) and Lecce (ECO). The location of Lampedusa (LMP) is also reported. The insert reproduces the WRF-Chem spatial distributions of surface O_3 mixing ratios (ppb) over the Mediterranean basin averaged over the period June – August 2010 (modified from Safieddine et al., 2014). The white box indicates the boundaries of the geographical map (courtesy of Google maps). The three I-AMICA observatories can provide continuous observations of RG and CH_4 variability in the central Mediterranean basin, a "hot-spot" region for air-quality and climate change. DOI: https://doi.org/10.1525/elementa.216.f1

at the three I-AMICA Observatories. The importance of these trace gases is well known and described elsewhere (e.g., Crutzen et al., 1999; Volz-Thomas et al., 2002; UNEP and WMO, 2011; Seinfeld and Pandis, 1998; Schultz et al., 2015; Ramanathan and Xu, 2010; Shindell et al., 2012). Even if no information about year-to-year variability can be provided by this work, significant preliminary information about RG and CH_4 variability in a still poor-investigated region are presented.

The next section presents the measurement sites both in terms of experimental set-up, environmental features, meteorological characterization and air mass synoptic scale circulation. Then typical levels and variability of the RG and CH_4 are analyzed and discussed. Finally, the comparison of surface O_3 and CO observations in Sicily (at CGR) with concurrent measurements at the GAW/WMO regional station of Lampedusa (LMP: 35.5182°N, 12.6305°E, 45 m a.s.l.), provides new preliminary hints on the impact of continental air mass outflow on surface O_3 variability in the central Mediterranean Sea.

2. Experimental

2.1 Measurement sites

To provide a general characterization of each measurement site, external views, wind roses and air mass 3D back-trajectories analysis (by Hybrid Single Particle Lagrangian Integrated Trajectory Model, HYSPLIT model; Stein et al., 2015) are reported in **Figure 2**. To depict the synoptic scale circulation affecting the I-AMICA sites, 5-day back-trajectories were calculated every hour with the HYSPLIT back-trajectories model (Draxler and Hess, 1998). The model calculations were based on the GDAS meteorological field produced by NCEP with a horizontal resolution of 1° × 1°. Sub-grid scale processes, such as convection and turbulent diffusion, were not represented by the model. To partially compensate such uncertainties, back-trajectory ensembles were calculated, with endpoints shifted by ± 1° in latitude/longitude. For each measurement site, **Figure 2** provides the "concentration field" of back-trajectory points over the whole investigation period.

Capo Granitola observatory (GAW ID: CGR, 37.66670°N 12.65000°E; 5 m a.s.l.) is located at the southern Sicily coastline facing the Strait of Sicily, at Torretta Granitola (12 km from Mazara del Vallo, 52,000 inhabitants), within the scientific campus of the Institute for the Marine-Coastal Environment (CNR-IAMC). This observatory carries out continuous atmospheric composition measurements well representative of western Sicily/central Mediterranean basin conditions. It frequently encounters air masses that are characteristic of background conditions in the Mediterranean basin (**Figure 2, A3**) and provide useful hints to investigate the influence of specific atmospheric processes (e.g. long-range air mass transport, mineral dust emitted from Northern Africa, anthropogenic ship emissions) when strong variability of tracers is encountered.

The CGR location is affected by the sea-land breeze regime, with prevailing (49% of hourly occurrence

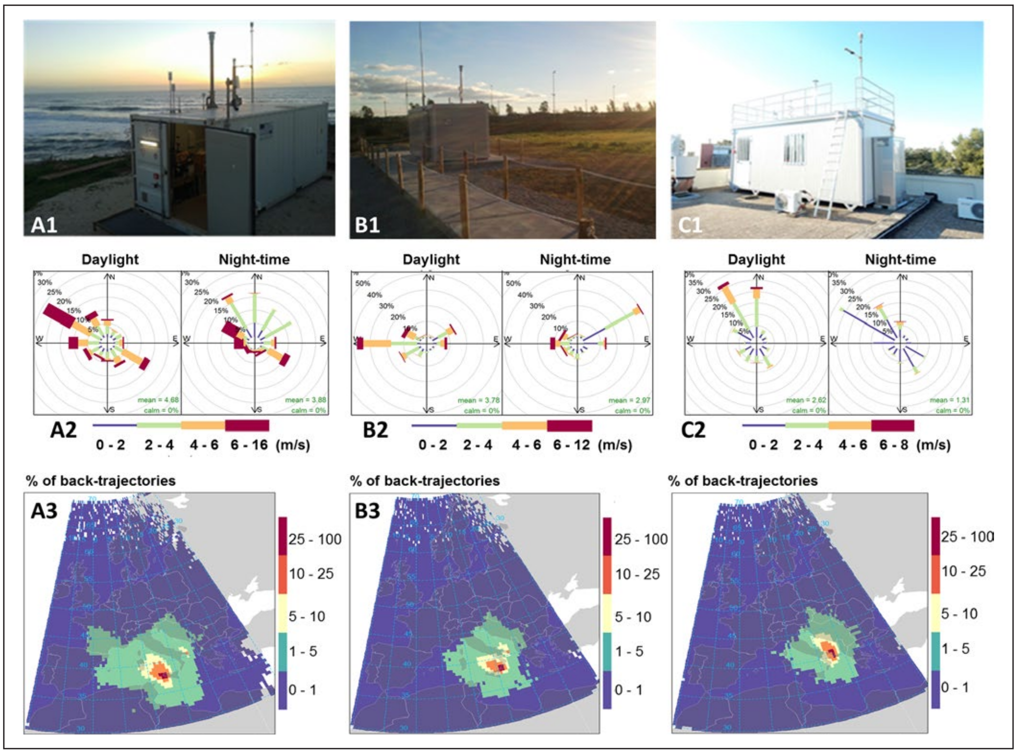

Figure 2: External views of observatories (1), daytime and nighttime wind roses (2) and gridded HYSPLIT back-trajectory frequency (3) for CGR (A), LMT (B) and ECO (C). Local air-mass circulation at CGR and LMT was strongly affected by the sea-land breeze wind regime. Synoptic-scale circulation was characterized by a main north-westerly flow at CGR and LMT, while north-westerly flows mainly affect ECO, as deduced by 5-day long HYSPLIT back-trajectories analysis. DOI: https://doi.org/10.1525/elementa.216.f2

throughout the measurement period) gentle wind breezes (up to 4 m/s) from inland (NW–NE) during the night and prevailing (80%) winds from the sea (W–SE) during daytime. The systematic occurrence of the breeze regime is also well-reproduced by the seasonal diurnal cycle of wind speed (Figure S1). On a seasonal basis, high water vapor values (obtained by the Cavity-Ring Down Instrument, see Section 2.2) were observed during summer, when a clear diurnal cycle with the highest value during daytime is also observed at the station. The overall back-trajectory frequency showed that CGR is strongly affected by air masses originating or passing above the central Mediterranean basin (Tyrrenian Sea), exhibiting a prevalent north-westerly circulation.

Lamezia Terme observatory (LMT, 38.87630°N 16.23220°E; 6 m a.s.l.) is located 600 m from the coastline of the Tyrrenian Sea. This region is characterized by anthropogenic pollution emissions related to transportation (airport, sea cruises from/to Gioia Tauro, local and highway vehicular traffic), domestic uses and agriculture. In particular, Lamezia Terme International Airport (14,699 flights in 2015) and the city of S. Eufemia (5,000 inhabitants) are located 5.5 km and 6.7 northward, respectively. The A13 motorway runs around the observatory location clockwise from N to S, and is located 7 km (northward) to 3.5 km (southward) from the observatory. HYSPLIT back-trajectory analysis showed a main westerly synoptic scale circulation during the investigation period. As depicted by local wind analysis, a breeze system also affects LMT. Moderate wind breezes from the sea (NW–SW) were mainly observed (55% of hourly occurrence) during daytime, while NE gentle wind breezes from land mainly (50% of occurrence) affected the nighttime period. The diurnal cycle of wind speed (Figure S1) is enhanced during summer when the synoptic scale forcing during nighttime (Federico et al., 2010) leads to higher wind speed. In agreement with CGR, a significant increase in the average water vapor concentration was observed at LMT from winter (by up to 1.5%) to summer (by more than 2.3%). During all the seasons (with a special emphasis in summer), daytime water vapor values appeared to be enhanced in respect to nighttime, exhibiting the impact of the sea breeze regime. At LMT, reactive gas observations have been fully operative since April 2015.

Lecce observatory (ECO, 40.33580°N 18.12450°E; 36 m a.s.l.) is located about 4 km (W–SW) from the urban area (94,148 inhabitants), at about 10 km from South Adriatic sea and can be classified as an "urban background" site (Contini et al., 2010). The site is located about 30 km and 80 km from the most important industrial centers of the Apulia Region (Taranto and Brindisi). The observatory is accommodated in a shelter located on the roof of the ISAC-CNR building (Division of Lecce), 12 m above the street, inside the University Campus (**Figure 2**). As highlighted by HYSPLIT back-trajectories analysis, a prevalent north-westerly circulation affected the measurement site region during the period of investigation (**Figure 2**). In agreement with Mangia et al. (2004), a complex system of sea-land breezes affected the region, leading to the occurrence of NW–SE light breezes during nighttime and NW–N moderate breezes during daytime (**Figure 2** and S1). The lower average wind speed observed at ECO, pointed out a much lower direct influence of the sea breeze regime at this measurement site, located 10 km from the coastline facing to the Adriatic Sea, compared to CGR and LMT. This is evident by the "reverse" diurnal variation of water vapor during summer (characterized by lower values during the central part of the day), indicating a prevalence of the dilution processes within the daytime well mixed PBL.

2.2 Sampling systems, instrumental set-up and quality check/quality assurance

At LMT and ECO the air intake for gas measurements is composed of a Teflon tube (length: 1300 mm), with a manifold of 50 mm inner diameter. An aluminum hood is used to prevent rain penetration inside the sampling intake. Air is sampled 1 m above the station roof (3.7 m from the ground at LMT and 15.7 m from the ground at ECO). The internal temperature is continuously monitored: to prevent water condensation the tubing is heated up to 27°C. Flow is maintained constant minimizing (below 5 s) the residence time of sampling inside the air intake.

At CGR, the air intake is composed of a Teflon tube (length: 2600 mm) with 50 mm inner diameter. An upper hood (Teflon-coated) is used to prevent rain penetration inside the sampling intake. Air is sampled 1.5 m above the station roof. Internal temperature and relative humidity are continuously monitored and temperature is keep 4ºC higher than ambient temperature to prevent condensation. Flow is maintained constant minimizing (below 5 s) the residence time of sampling inside the air intake. Flow as well as internal T and RH are continuously monitored and recorded by the acquisition system.

At all the measurement sites, ¼" (OD) Teflon© tubes (Synflex 1300 tubes for cavity ring-down absorption spectrometry, CRDS, measurements) are used to connect the air intake manifold with gas analyzer particulate filters (Teflon©) present at the instrument inlet (changed every 30 days).

Surface O_3 (CGR, LMT, ECO): Instruments (UV-absorption analyzer Thermo 49i) are equipped with an internal span source (ozonator) and external zero source (purafill filled cartridge) which allow the daily execution of zero/span checks. Instruments are calibrated in situ on a yearly basis against a traveling calibrator (Thermo 49iPS, S/N 1425162559) hosted at the Lecce observatory. The travelling calibrator (TC) was compared against the standard reference SRP15 hosted at the GAW WCC at EMPA in July 2015. The agreement between SRP15 and the I-AMICA TC was excellent and the following calibration function was determined for the range 0–250 ppb: $[O_3]^{SRP15} = ([O_3]^{TC}+0.04 \text{ ppb}) / 0.9987$. At CGR and ECO, surface O_3 measurements have been available since January 2015, at LMT since April 2015.

NO and NO_2 (CGR, LMT, ECO): Instruments (Thermo 42iTL) are checked monthly against zero and span checks using external zero air generators (Thermo 1160) and gas dilution/GPT systems (Thermo 160i). NO span and evaluation of converter efficiency by GPT are carried out using a certified 5 ppm NO standard (in N_2) provided by commercial laboratories (Praxair, Rivoira and Messer Italia). To carry out calibration procedure the methodology recommended within the ACTRIS EU project was implemented (see Gilge et al., 2014). The ~5 ppm NO standard is diluted to a 100 ppb level and used to determine the NO span factor. Then GPT is used to titrate about 80% of the NO amount obtained by dilution: this allow to determine the NO_2 to NO conversion efficiency. The instruments are challenged by zero air (obtained by a dry air generator equipped with adsorbent traps) at the beginning and at the end of the calibration procedure. Over one year period the zero factor ranged from –0.03 ppb to 0.02 ppb, the NO span factor from 0.961 to 1.059, while the conversion efficiency ranged from 0.987 to 0.956. These checks were carried out every two months at CGR and every 6 months at LMT and ECO: the obtained calibration coefficient were used to correct the obtained raw mixing ratios. Multipoint calibrations by NO dynamic dilution is carried out at CGR on a yearly basis to evaluate instrument linearity over a range from 1 – 20 ppb. At CGR, the laboratory standard have been also compared with the NO standard available at the Monte Cimone WMO/GAW Global Station (GAW ID: CMN), Italy. In March 2013, the CMN NO standard (5.28 ppm) participated to a round robin test executed in the framework of the ACTRIS Project. A NO (2.07 ppm) in N_2 mixture was purchased from NPL and used as ACTRIS test gases. All the instruments are equipped with a standard heated (300°C) Molybdenum converter. As indicated by Steinbacher et al. (2007), the NO_2 readings can be overestimated by up to ~50% due to the interference of other oxidized nitrogen compounds such as peroxyacetyl nitrate (PAN) and nitric acid: this limitation will be considered in the data discussion. Fitting the instruments with photolytic converters is planned. A detection limit of 0.05 ppb was experimentally assessed for the I-AMICA instruments on a 1-minute basis. At CGR, NO and NO_2 values have been available since February 2015, at LMT since April 2015. Due to instrument problems, no NO and NO_2 data are available at ECO for the period of investigation. No correction for water vapor (WV) or O_3 interferences on NO and NO_2 readings were applied to the analyzed data-set. The WV interference, due to quenching effect in the CLD reaction chamber, can introduce a bias in NO reading up to 15% under warm (i.e. T = 30°C) and humid (RH = 80%) ambient conditions. Since along the sampling line the NO_2 photolysis is stopped whereas the reaction of NO and O_3 continues, an overestimation of NO_2 and underestimation of NO is expected to occur. For residence time of 5 sec inside the inlet (at 25°C and 1013 hPa), the underestimation for NO can be up to 20% of the instrument reading (for O_3 concentration of 70 ppb), while the NO_2 overestimation can reach up to 3% for NO_2 value of 2 ppb and NO of 0.4 ppb.

SO_2 (CGR): The instrument (Thermo 43iTLE) is equipped with an internal span source (permeation tube) and external zero source (activated charcoal filled cartridge) which allow the daily execution of zero/span checks. A dilution system (Environics 4000) is available to perform every 6 months multi-point calibration (range: 0.5 – 10 ppb) from a certified 235 ppb SO_2 standard (s/n: 12048642) provided by Rivoira (expanded uncertainty with coverage factior k = 2, 35 ppb). A detection limit of 0.17 ppb was experimentally assessed for the CGR instrument on a 1-minute basis. SO_2 observations have been available since January 2015.

CH_4 and CO: Cavity ring-down spectrometers (Picarro G2401) are connected by Synflex 1300 tubes (OD: ¼") to the air intake manifold. A set of n.3 calibration standards from NOAA-GMDL is available at the LMT station: CB11039, CB11164, CB10928. They represent the I-AMICA "primary" standards. During the period of investigation, routine calibration (every 48h at LMT, every month at CGR and ECO) was carried out using observatory working standards (for each gas, two working standards with CH_4, CO_2 and CO mixing ratios representing upper and lower ranges of the expected ambient variability were used) to evaluate possible drifts and the stability of calibration factors. CGR working standards were compared against LMT NOAA standards, while at ECO calibration were only performed against the available commercial standards. This means that a special caution would be deserved in comparing ECO observations with that obtained at LMT and CGR. Moreover, in the framework of QA/QC activity, a round robin program between LMP and CGR was started on 2016. Due to the high water vapor concentrations usually affecting the I-AMICA measurement sites, the correction coefficients determined by Chen et al. (2010) were applied to partially correct the effect of water vapor on CO_2 and CH_4. Specific tests (see Rella et al., 2013 and Zelwegger et al., 2012) are ongoing to completely characterize proper instrument operation as a function of different WV ranges. The results of these tests were not implemented to the data series here reported. Data are recorded on a 5 s basis by the Picarro internal PC and mirrored to a station server, then delivered in NRT mode to ISAC-CNR HQ in Bologna, where 1-minute averages were calculated. On an hourly basis data were flagged to avoid local contamination by excluding data with hourly CH_4 standard deviations exceeding 60 ppb. CRDS observations have been available since January 2015 at ECO, March 2015 at CGR and April 2015 at LMT.

For all the instruments and observatories, information on instrument functioning and maintenance interventions are stored in an e-logbook. For all the gas measurements, 1-minute data and metadata (internal parameters: fluxes, lamp intensities, PMT voltages, chamber pressures, bench temperatures…) are visually inspected on a daily basis by an HTML page reporting the last 48h of available measurements and instrumental internal parameters. Final aggregation to hourly average will be executed using validated 1-minute data. Data and metadata are analyzed on a monthly basis. Quality assurance procedures involve time series plots, consistency checks on co-variability among gas parameters, meteorology and aerosol properties.

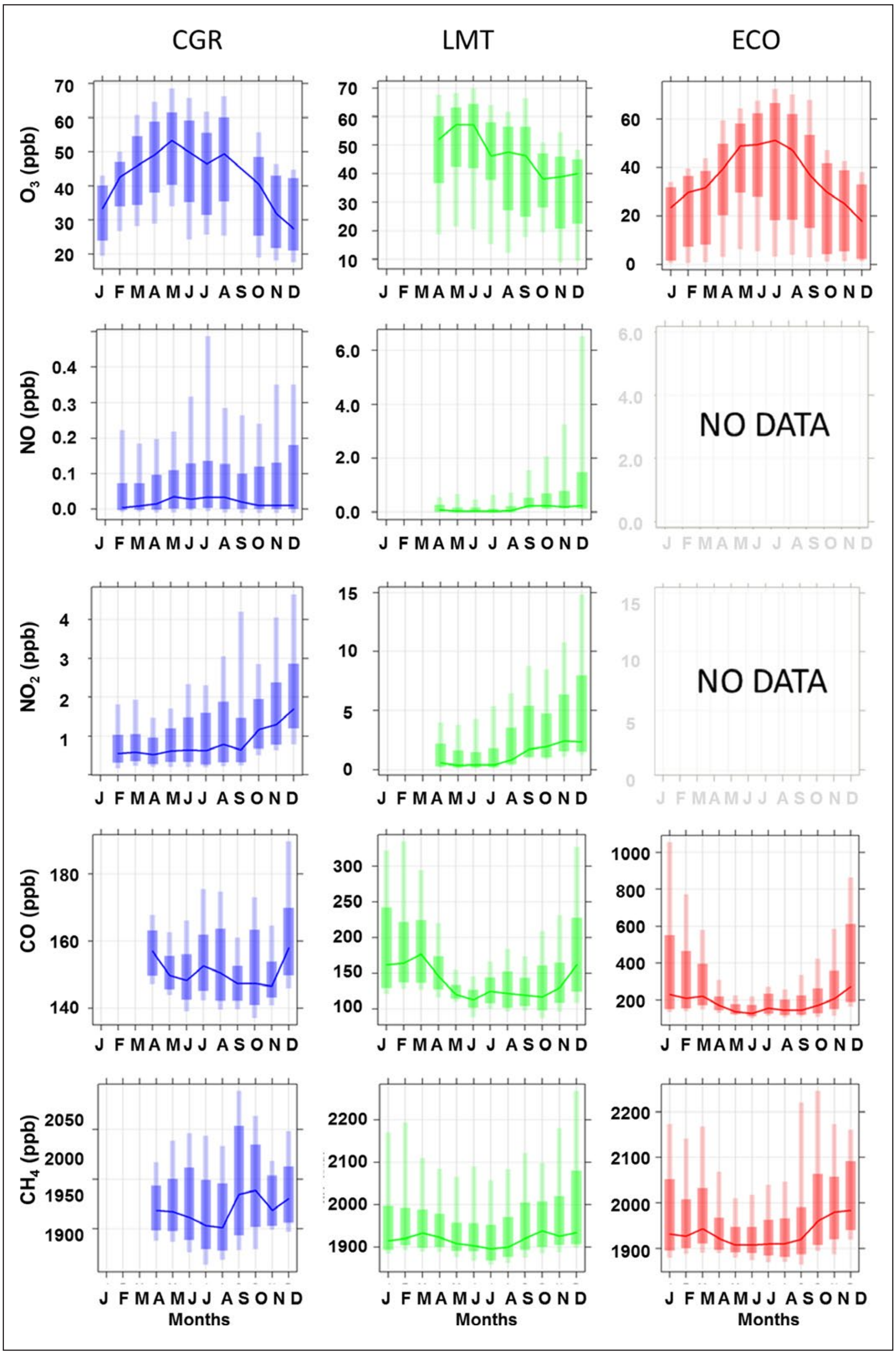

Figure 3: Comparison of the RG and CH_4 values at the three I-AMICA observatories. The plots report monthly medians (continuous line) and percentiles (10^{th}, 25^{th}, 75^{th} and 90^{th}) for hourly values of RG and CH_4 at the three I-AMICA observatories (CGR: blue, LMT: green, ECO: red). DOI: https://doi.org/10.1525/elementa.216.f3

3. Results and discussion

In this Section, RG and CH_4 data for CGR, ECO and LMT were discussed in terms of monthly (**Figure 3**) and hourly (**Figure 4**) variabilities. For what concerns typical diurnal variations, the confidence interval (at the 95%) were calculated by using the R package "Openair" through bootstrap re-sampling, which will provide better estimates than the application of assumptions based on normality (see Carslaw, 2015).

3.1 Trace gas variability at CGR

The surface O_3 hourly values (yearly mean average value: 55.3 ± 0.9 ppb) were characterized by an evident seasonal cycle with winter minima and highest values in May and August (**Figure 3**). During winter–autumn, the monthly 10th percentiles did not decrease below 20 ppb, while during warm months the 90th percentiles did not exceed 65 ppb, which can be considered indicative of the low impact of NO titration during cold months and photochemistry production in summer. Indeed, low mean average values were observed for NO and NO_2 (0.05 ± 0.01 ppb and 0.94 ± 0.02 ppb, respectively), which are characterized by higher values of median and upper percentiles during cold months (October – December) and summer (June – August). This was true especially for NO. The summer increase is rather unexpected for NO and NO_2 due to their short atmospheric lifetimes in summer, as also reported by other studies in the Mediterranean region (e.g. Boersma et al., 2009). Even if the low mean average values suggest that CGR is not heavy impacted by "fresh" anthropogenic emissions, the summer increase of CO (**Figure 3**) and NO/NO_2 (Figure S2) suggested a seasonal trend in the local/regional emissions, probably related to tourist activities (i.e. vehicular traffic). For instance, the total population of Mazara del Vallo (12 km from CGR) increased by more than 35% during the summer months compared to winter–spring.

For CO (average value: 130.2 ± 0.7 ppb) we did not observe a clear seasonal for the monthly medians and percentiles. Indeed a secondary peak in summer (July – August) was observed at CGR (both on median and upper percentiles), while the highest hourly values were detected in December. This behavior is rather different from the typical CO annual cycles presented in previous studies for background or remote sites (e.g. Novelli, 2003; Gilge et al., 2010) characterized by minima in summer and peak in winter-spring. This can be due to the lack of observations during the first three months of the year, which prevent any conclusive analysis of the spring period, and to the regional increase of anthropogenic emissions during the summer or other contributions (e.g. long-range transport of biomass burning emissions). With the aim of shading light on anthropogenic emissions contributing to CO variability, we calculated the hourly CO/NO_x ratio (Figure S3), since this parameter can be used to attribute CO emissions to motor vehicular exhaust or other sources. However, it should be considered that several factors related to different emission sources or air-mass aging, photochemistry, mixing or dilution can affect ambient CO/NO_x (Li et al., 2015). The monthly evolution of CO/NO_x, showed higher values from April to September, while the lowest CO/NO_x (median values ~ 100 ppb/ppb, 75th and 90th percentiles lower than 200 ppb/ppb) were observed in October – December. Probably, this yearly behavior stress the influence of a more mixed/diluted PBL and a higher NO_x degradation by OH. However, even the lowest CO/NO_x values observed during cold months suggested only a limited direct influence of "fresh" vehicular traffic emissions (Li et al., 2015). More years of measurement are needed to understand if this represents a typical feature at this measurement site.

The CH_4 (average value: 1925.3 ± 1.0 ppb) monthly median values and 10th – 25th percentiles were lower in July – August than in April – June and September – October, probably due to the more efficient oxidation by OH during summer months.

For a considerable fraction of the investigated period, SO_2 was below the detection limit at CGR (average value:

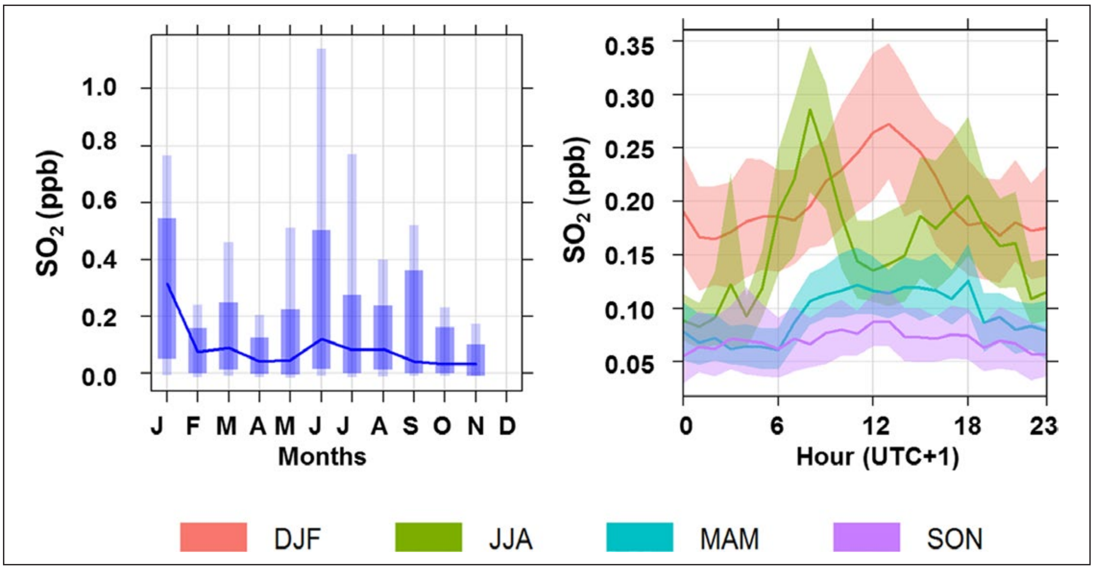

Figure 4: SO_2 variability at CGR. Right: monthly medians (continuous line) and percentiles (10th, 25th, 75th and 90th) for hourly values of SO_2 at CGR. Left: seasonal average diurnal variations. The dashed areas represent the 95% confidence interval. High SO_2 values were observed in winter (daytime) and in summer (early morning and evening). DOI: https://doi.org/10.1525/elementa.216.f4

0.10 ± 0.01 ppb), thus special caution is needed in commenting on the SO_2 results (**Figure 4**). SO_2 monthly values showed no evidence of a seasonal cycle at CGR. Peak values of monthly median and upper percentiles were observed in January (median value: 0.32 ppb) and June (0.10 ppb) related to the occurrence of long-lasting "enhanced" SO_2 episodes (1–20 January and 1–17 June 2015). During January, the episode occurred under high pressure conditions with low wind speed regimes (lower than 5 m/s). The analysis of SO_2 hourly variability as a function of wind direction pointed out that during daytime the highest SO_2 values (higher than 0.4 ppb) were mostly related to air from sea (westerly winds), while during night-time they were related to air-masses from inland (northerly winds) . Also during the June 2015 episode, the highest SO_2 values (higher than 0.5 ppb) were observed under "light air" to "gentle breeze" conditions (i.e. wind speed lower than 5 m/s) characterized by relatively dry conditions (RH lower than 70%) and air-temperature increases (up to 25°C).

Further hints towards a better understanding of the processes driving the variability of the observed atmospheric compounds can arise from the analysis of the typical seasonal diurnal variations (**Figure 5**). Seasonally averaged diurnal O_3 cycles were characterized by higher values during the central part of the day and minima during nighttime. The highest cycle amplitude was observed in summer (30 ppb) and the lowest in winter (18 ppb).

The NO seasonal diurnal variations were characterized by a peak in the early morning (time window: 6 – 8), which is likely to trace the rush hour emissions within the shallow coastal PBL, while very low NO values were observed during nighttime due to NO removal by O_3 and air-mass mixing. The magnitude of the morning NO peak was larger in summer and autumn: again, this suggested an increased influence of anthropogenic emissions (probably related to vehicular traffic) during warm months, due to tourist activities in the region, even if a role of enhanced NO_2 photolysis cannot be neglected. Moreover, during summer a significant NO peak was evident during the evening, further supporting increased traffic emission in summer. The predominant influence of anthropogenic activities (e.g. traffic) as an NO source can be identified by the one hour shift of the morning peak when moving from winter to spring due to the introduction of daylight saving time, occurring in Italy on the last Sunday of March. Statistically significant ($p < 0.05$) higher NO values affected the measurement site during daytime (under sea breeze regime) in comparison to nighttime, indicating a not completely negligible presence of NO within air-masses affected by sea breezes towards the Sicily coastline (possibly exhibiting off-shore emissions by ships).

NO_2 seasonal diurnal cycles were characterized by a peak in the early morning, a minimum during daytime and a peak during the evening (18 – 23). The early morning peak (statistically significant only in spring and summer) is coincident with the NO peak and it occurred earlier in summer than in autumn–winter. The daytime values are minimized during spring and summer, pointing towards more efficient NO_2 photolysis, photo chemically driven oxidation processes and air-mass mixing under well-developed PBL. The evening peak is maximized in winter and autumn: the low NO/NO_2 values tagged these high NO_2 values to emissions transported from the interior to the measurement site (Figure S2).

CO seasonal average diurnal cycles (**Figure 5**) showed a shape similar to NO_2 (high values during nighttime/early morning, daytime minima and increasing values in the evening). However, except that in winter and summer, we observed comparable CO values throughout the 24 hours (not statistically different at the 95% confidence level). In winter, very large CO peaks were observed in the early morning and during evening/night. During summer, we observed significant ($p < 0.05$) lower values during daytime, when the influence of sea breeze circulation and photochemistry is maximized at the measurement site. In the other seasons, the absence of clear diurnal cycles was due by superimposed contributions of different source types. The flat average diurnal cycles observed from spring to autumn, were probably mostly due to weaker inversion layer and enhanced vertical mixing within the coastal PBL.

As for other primary pollutants, the CH_4 diurnal cycles (**Figure 5**) were characterized by high values during nighttime/early morning, and minima in the central part of the day. This cycle amplitude is maximized in spring–summer, when the differences between nighttime and daytime values become statistically significant. The small differences between nighttime and daytime values during winter-autumn, suggested only limited anthropogenic CH_4 emissions at local/regional scale. Moreover, the lack of statistically significant seasonal variation of night time CH_4 could point to constant sources throughout the year. Interestingly, on average, no significant early morning peaks were observed for CH_4, further stressing the role of traffic as responsible for the occurrence of the early morning peak for CO and NO_x. Daytime values decreased from winter to summer and increased again during autumn. This provided hints that OH induced depletion of CH_4 is the main process determining the observed diurnal behavior in addition to diurnal increase/decrease of mixing height.

The SO_2 seasonal average diurnal cycles (**Figure 4**) were characterized by the occurrence of peaks during the central part of the day in winter (but not statistically significant at the 95% confidence level) and spring, which can be tentatively related to the occurrence of marine biogenic and/or anthropogenic ship emissions. Indeed, a similar diurnal cycle was observed by Yang et al. (2016) at a coastal location in the North Sea and attributed to the photo-oxidation of biologically derived dimethyl sulfide (DMS), which represents a major pathway for SO_2 production in the marine environment. When, using HYSPLIT back-trajectories, we selected the measurement periods characterized by air-masses only travelling over sea surface before reaching CGR (here not shown), an increase of the winter spring peak was observed (hourly peak value above 0.5 ppb). This would further stress towards a role played by marine emissions in the appearance of the winter diurnal peak. Unfortunately, no concurrent observations of NO_x or CO were available at CGR in January – February when the

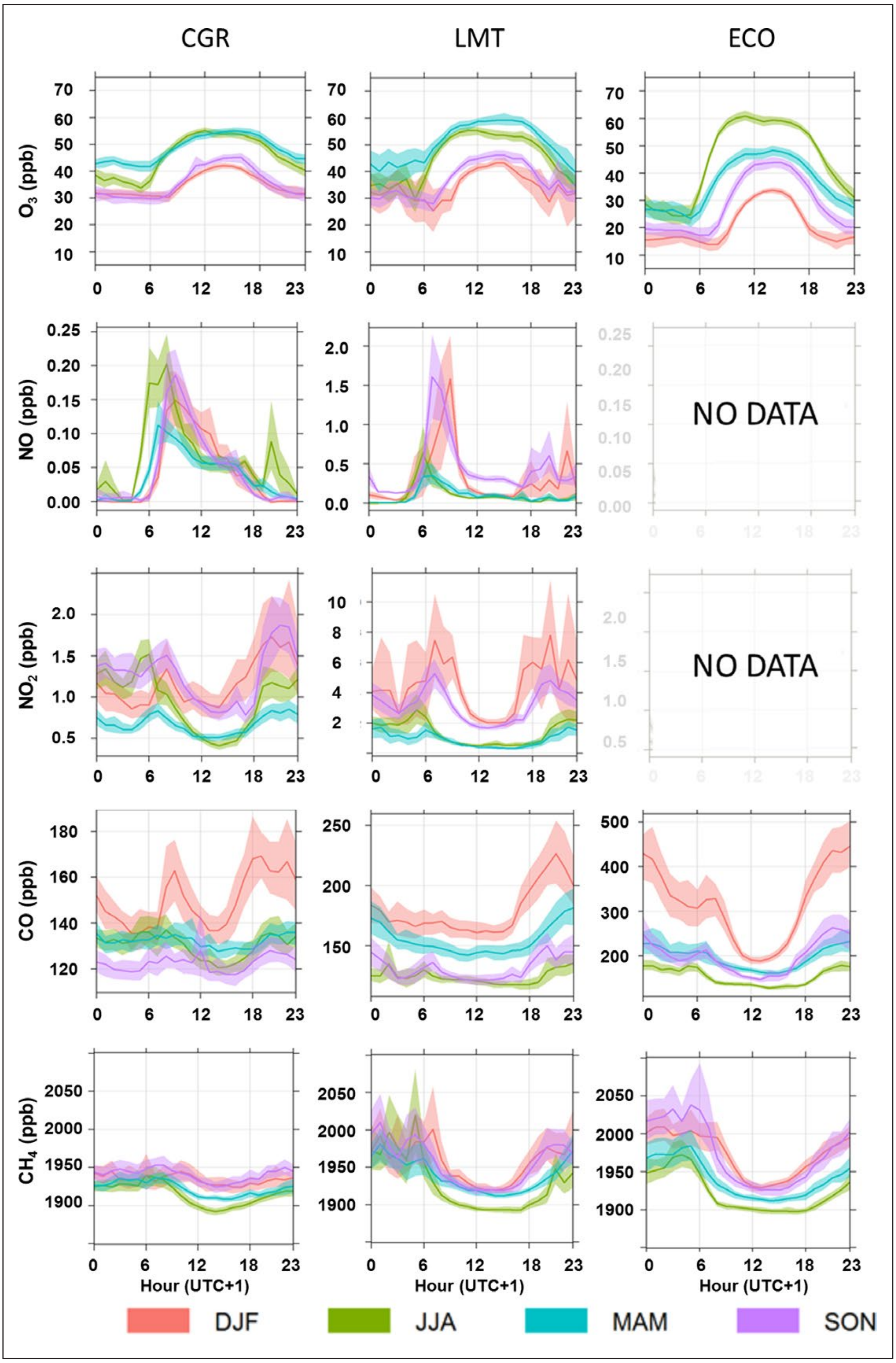

Figure 5: Typical seasonal diurnal variability of RG and CH_4 at the tree I-AMICA observatories. Seasonal average diurnal variations of O_3, NO, NO_2, CO, CH_4 at CGR, LMT and ECO. The dashed areas represent the 95% confidence interval. Please note the different scales for y-axes as a function of the measurement site. DOI: https://doi.org/10.1525/elementa.216.f5

highest SO_2 levels were observed. Thus, a definitive attribution of the high SO_2 values (well above the instrumental detection limit) observed during daytime in January to DMS oxidation or to anthropogenic (ship?) emissions is challenging. However Lana et al. (2011) suggested that DMS emissions are minimized over Mediterranean during winter (thus supporting a role of ship emissions for the high winter SO_2 values at CGR). More analyses and a longer data-set is needed to better disentangle this point. An evident feature in the SO_2 diurnal cycle is the occurrence of a morning (6 – 10) peak in summer, which perfectly matches the NO diurnal peak and may reflect the larger anthropogenic emissions during these months under land breeze circulation and shallow boundary layer heights. Similarly to what observed for NO, a significant SO_2 decrease (but with still detectable SO_2 loading) was then observed during daytime (minimum values at noon), when sea breeze affected CGR.

3.2 Trace gas variability at LMT

The surface O_3 hourly values (average value: 44.2 ± 0.4 ppb) were characterized by higher values in spring-summer. At LMT, yearly average values were 0.31 ± 0.02 ppb and 0.69 ± 0.01 ppb for NO and NO_2, respectively. As reported in **Figure 3**, much larger variability affected NO and NO_2 at LMT in comparison with CGR, especially during autumn-winter when higher upper percentiles were reported. In fact, a clear seasonal cycle is discernible at LMT for NO and NO_2 upper percentiles, with increasing values from summer to winter, when the highest monthly mean values (0.82 ppb and 4.04 ppb for NO and NO_2, respectively) were observed. The NO/NO_2 values at LMT showed much higher values than at CGR (roughly a 3-fold increase), indicating the larger impact of more "fresh" anthropogenic emissions. On a monthly basis, the seasonal cycle was enhanced for the upper percentiles (peak values during cold months and minima during summer), due to the lower lifetime of NO during the summer months.

The analysis of the monthly CO percentiles at LMT (average value: 146.1 ± 1.1 ppb) revealed high values during winter and spring (**Figure 3**). CO at LMT approached the values observed at CGR only during summer, while they were much more higher in winter and spring, indicating a larger impact of combustion sources. It is interesting to note that the increase of the upper CO percentiles observed at CGR in July – August was also detected at LMT, thus suggesting that this is a regional feature, at least for year 2015. The higher CO values in winter were caused by increased anthropogenic emissions due to domestic heating and longer CO lifetime due to low OH in winter months (Schultz et al., 2015). The analysis of CO/NO_x (Figure S2) showed higher values from April to July. In particular, the most part of the hourly observations were lower than 100 ppb/ppb in winter/autumn, with minima (around 30 ppb/ppb), possibly exhibiting the influence of traffic emissions. The highest CO/NO_x values (median values higher than 200 ppb/ppb) were observe during spring-summer, exhibiting the advection of air-masses subjected to significant photochemical processing (Morgan et al., 2010). This was also evident for CH_4, (average value: 1938.1 ± 1.8 ppb) showing summer minima and winter-spring maxima. As for CO, NO_2 and NO, the CH_4 seasonal variability is much more evident for the upper percentiles than for the lowest ones, indicating the increasing impact of anthropogenic emissions during cold months together with the less efficient removal by OH. A significant correlation existed considering the daily average value of CO and CH_4 at LMT (R: 0.71), suggesting co-emissions by urban/industrial sources.

Surface O_3 showed seasonal diurnal shapes very similar to CGR (**Figure 5**), but with cycle amplitudes ranging from 12 ppb (winter) to 25 ppb (summer). Along the 24 hours, very small differences were observed between winter vs. autumn and spring vs. summer. It is interesting to note that, in agreement with CGR, the highest diurnal values were observed during spring afternoon (around 17), under the occurrence of sea breeze regime. As also proposed by Martins et al. (2012), air-masses advected by sea breeze towards the coastline can be relatively rich in O_3 due to the absence of NO titration during night-time within the marine boundary layer (MBL) and limited dry deposition over sea water. Once the sea breeze propagated inland, entrainment processes of air-masses from aloft can also represents a further O_3 source at the coastal surface. Interestingly, at CGR and LMT night-time O_3 was lower for summer in respect to spring. This may be the effect of the increased regional anthropogenic emissions during this season (see Section 3.4), which leaded to enhanced nigh-time titration by NO.

The NO seasonal average diurnal variations at LMT (**Figure 4**) were characterized by a peak in the early morning (7 – 8), which is likely to trace the rush hour emissions within the shallow coastal PBL, while very low NO values were observed during nighttime due to NO removal by O_3. As already observed at CGR, the magnitude of the morning NO peak increased sharply during summer: this suggested an increased influence of anthropogenic emissions (probably related to vehicular traffic) to NO variability during warm months, due to tourist activities in the region. However, the morning peak is maximized (4.7 ppb) in winter (December), as expected due to increase NO lifetime during cold months and more stable PBL conditions in the region (Federico et al., 2010). For all the seasons, after the onset of the sea breeze, decreasing NO values were observed until 12, followed by stable values close to detection limit until 18, when the land breeze usually start to affect LMT. This indicated, similarly to CGR, a not completely negligible presence of NO within air-masses affected by sea breezes towards the Calabria coastline, possibly indicating a role played by off-shore ship emissions. This is not unconceivable, since Gioia Tauro, the most important port for commercial shipping in the central Mediterranean basin, is located 72 km from LMT. NO_2 seasonal diurnal variations peaked during night-time/early morning (with the highest values in autumn-winter), while lower values (about 0.5 ppb in spring-summer and 2.0 ppb in autumn-winter) were observed during day-time (under sea breeze circulation). As for NO, the time duration of the NO_2 morning peak appeared to be modulated by the onset of the sea breeze: in autumn-winter, the delayed sea breeze onset leaded to a longer duration of the early morning peak.

The CO seasonal diurnal variations (**Figure 4**) were characterized by lower values during daytime and higher values during nighttime. This can be explained considering the accumulation of CO during nighttime under stable boundary layer conditions and the occurrence of sea breeze during daytime. The evening CO peak, associated with the occurrence of land breeze circulation is maximized in winter. Moreover, during summer, daytime average CO values were not statistically different (at the 95% confidence level) between CGR and LMT, supporting the view that when sea breeze affects these measurement sites, the observations were well representative of the regional background. Indeed, CO at LMT and CGR showed a significant correlation on a daily basis (R: 0.51). Even considering the spatial distance between these two observatories (more than 300 km), this would indicate that CGR and LMT were affected by synoptic air masses (see HYSPLIT analysis by **Figure 1**) with similar CO fingerprints, more representative of the central Mediterranean background.

At LMT, the CH_4 diurnal cycles appeared to be enhanced in respect to CGR, with higher values during nighttime (not varying with the seasons) but comparable low values during daytime. This clearly indicated higher CH_4 emissions occurring at regional scale and transport by nighttime land breeze towards the measurement site. During nighttime (0–6), no different CH_4 values were observed as a function of the season: this point to constant CH_4 sources throughout the year. Moreover, the nighttime peak in CH_4 was not reflected by CO observations: this would indicate substantial CH_4 emissions not related to combustion processes for this region (e.g. stock lives, agriculture, waste management).

3.3 Trace gas variability at ECO

At ECO, the seasonal cycle of surface O_3 (average value: 32.9 ± 0.4 ppb) was characterized by a broad spring-summer maximum and a winter minimum for the monthly median and the upper percentiles (**Figure 3**), typical for sites affected by local anthropogenic emissions. Among the three measurement sites, at ECO we observed the lowest monthly percentiles of the hourly O_3 values, indicating efficient night-time NO titration, especially in winter-autumn when the monthly 25th percentiles did not exceed 10 ppb.

The analysis of monthly percentiles of hourly CO values (average value: 215.7 ± 3.0 ppb) revealed high values for median and upper percentiles during January – March and November – December (**Figure 3**), indicating a larger variability of hourly CO values in respect to LMT and CGR. In April – August, both average/median values and variability (traced by the inner quantile) decreased, approaching the values observed at CGR. However, even during warm months, CO values were higher at ECO, indicating a larger impact of urban combustion sources.

For CH_4 (average value: 1952.6 ± 1.8 ppb) high hourly values were observed in January – April and October – November, predominantly. With respect to CO (**Figure 3**), CH_4 variability at ECO appeared to be more comparable to LMT, even if ECO was affected by occurrence of higher CH_4 values, as deduced by the larger 75th and 90th percentiles in January – March and October – December, clearly indicating a larger impact of direct emissions. A significant correlation characterized the time series of daily CH_4 values at the three measurement sites (R: 0.33 at ECO and LMT and R: 0.32 at LMT and CGR), probably due to the long tropospheric lifetime of CH_4. Nevertheless, at ECO, CH_4 peaks exceeding 2000 ppb were often observed in coincidence with CO increases (not shown), and the significant linear correlation between daily CH_4 and CO (R: 0.67) suggests co-emissions by urban/industrial sources.

Among the three sites, ECO showed the largest diurnal O_3 cycle amplitudes, with values ranging from 15 ppb in winter to 35 ppb in summer (**Figure 5**). This is not surprising, considering the proximity of ECO to the Lecce urban area. The increase of the diurnal cycle amplitude at ECO from winter to summer was mostly related to the increase of the daytime peak values even if the high nighttime CO could support strong NO titration impact (unfortunately NO observations were not available at ECO for the investigated periods).

Also at ECO, the CO seasonal diurnal variations (**Figure 5**) were characterized by lower values during daytime and higher values during nighttime. Despite LMT, night-time (0 – 6) CO values were comparable to the evening peak. With respect to LMT, this would indicate more diffuse CO sources in the Lecce urban area that, together with a more stable nightime "continental" PBL, could lead to these very high CO values. Interestingly, despite to what observed for CO, at ECO night-time CH_4 values were similar to LMT (**Figure 5**): for ECO this suggested co-located CO and CH_4 emissions. Irrespective of the season, the lowest differences between the three measurement sites were found during daytime (12 – 18) for CH_4. In addition to a likely role played by increased OH oxidation during daytime, this behavior further stresses that the measurement sites are more representative of the regional background conditions when air masses are flowing from the sea (for CGR/LMT), or when vertical mixing within the PBL and entrainment processes from free troposphere are maximized (at ECO).

3.4 Investigation of "photochemical age" at CGR and LMT

To investigate the impact of anthropogenic emission ageing to trace gas variability at CGR and LMT, we investigated the variability of hourly O_3 as a function of NO_x and CO for the different seasons (**Figure 6**). At CGR, irrespectively by the seasons, the highest O_3 values were observed with low CO and NO_x, exhibiting the occurrence of "background" air-masses. This regime appeared to be particularly relevant in spring and to lesser extent in summer. Low O_3 were mostly associated with high CO and NO_x, suggesting the occurrence of more "fresh" pollution emissions: this regime is particularly evident in winter and, to lesser extent, in summer and autumn. During summer and spring at CGR and summer and autumn at LMT, high O_3 values were also related with high CO and low NO_x, prob-

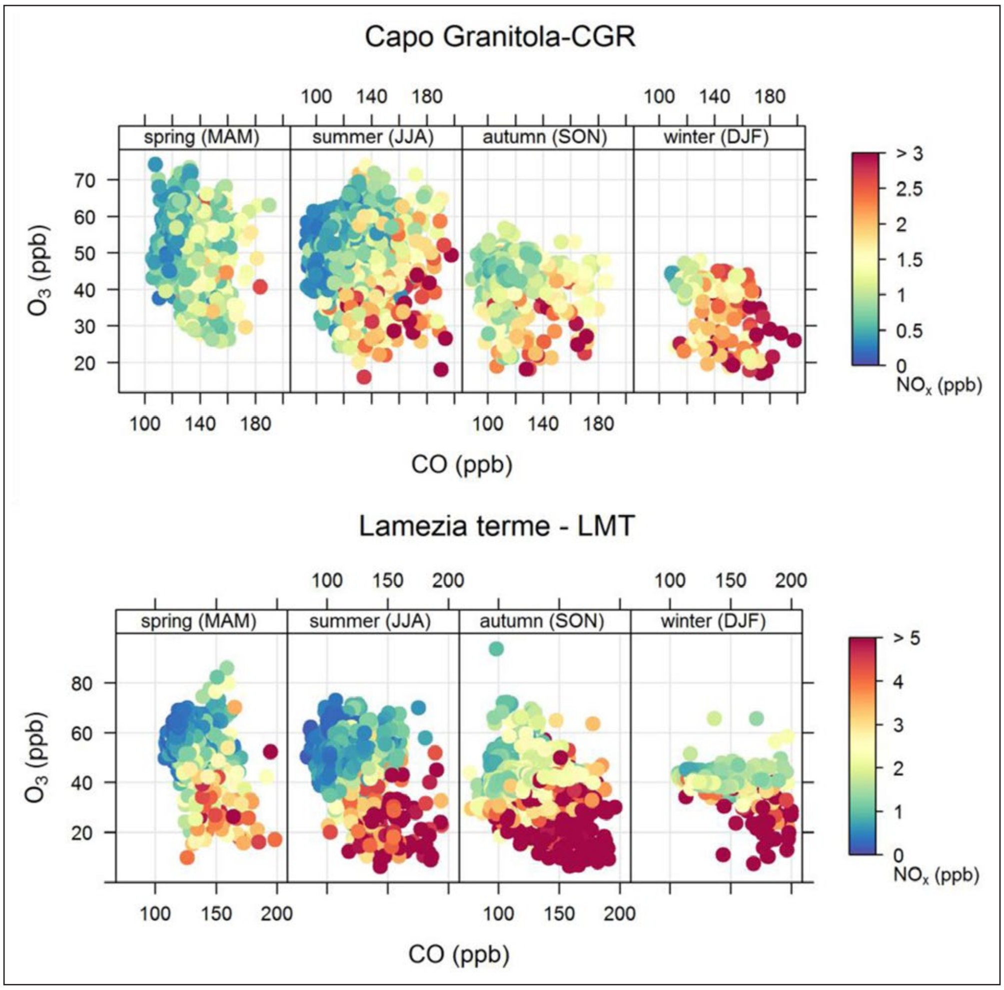

Figure 6: Scatterplot of hourly values of CO and O_3 at CGR (upper plate) and LMT (bottom plate) as a function of NO_x (colored code) for the different seasons. As deduced by the relationship of hourly O_3, CO and NO_x, CGR appeared to be particularly affected by "background" air-masses in spring and summer. The occurrence of more "fresh" pollution emissions was important in winter and, to a lesser extent, in summer and autumn. At LMT, the "fresh" pollution regime appeared to be more relevant during all the seasons. DOI: https://doi.org/10.1525/elementa.216.f6

ably indicating the occurrence of "aged" pollution. Similar features can be recognized also for LMT, but the "fresh" pollution regime appeared to be more relevant during all the seasons. Compared to CGR, a lower occurrence of "aged" anthropogenic emissions (i.e. high O_3, high CO and low NO_x) appear to affect LMT. This behavior is conceivable at LMT, considering that when air-masses is flowing from the land interior they were affected by anthropogenic emissions occurring in the Calabria region, while under sea breeze regime, air-masses more representative of the background conditions could be observed.

To provide a better assessment of the impact of air-masses with different anthropogenic emission aging at CGR and LMT, we investigated the variability of O_3/NO_x ratio that according to Morgan et al. (2010) and Parrish et al. (2009) can be considered proxies to qualitatively evaluate the proximity to major emission sources and photochemical processing.

According to Parrish et al. (2009) and Morgan et al. (2010), observations with $O_3/NO_x < 10$ (4 % and 20 % of data at CGR and LMT, respectively) can be considered representative of local emissions (LOC), $10 < O_3/NO_x \leq 50$ indicates nearby sources (39% and 40%, respectively), $50 < O_3/NO_x \leq 100$ (31% and 14%) applies to remote sources, while $O_3/NO_x > 100$ indicates processed air masses likely representative of the atmospheric background (26% for both the sites). The analysis of O_3/NO_x as a function of local wind direction (**Figure 7**) clearly underpins the role of the sea breeze in favoring the occurrence of "background" observations at CGR and LMT. In particular, during all the seasons, the lowest O_3/NO_x values at CGR were observed in concomitance with nighttime northerly winds from inshore, while higher ratios were observed with winds from the open sea (NW–SE). In particular, average O_3/NO_x ratios of 140 (50), 145 (45), 50 (10) and 75 (25) were observed for wind from off-shore (inshore) for spring, summer, autumn and winter. A similar situation is evident at LMT, where the lowest O_3/NO_x values (representative of local emissions) were related to land breeze, while O_3/NO_x higher than 100 were solely associated with sea breeze.

To entertain the possibility that the Mo detector used in the NO-NO_2 chemioluminescence analyzers could overestimate NO_2 readings for relatively aged air masses (see

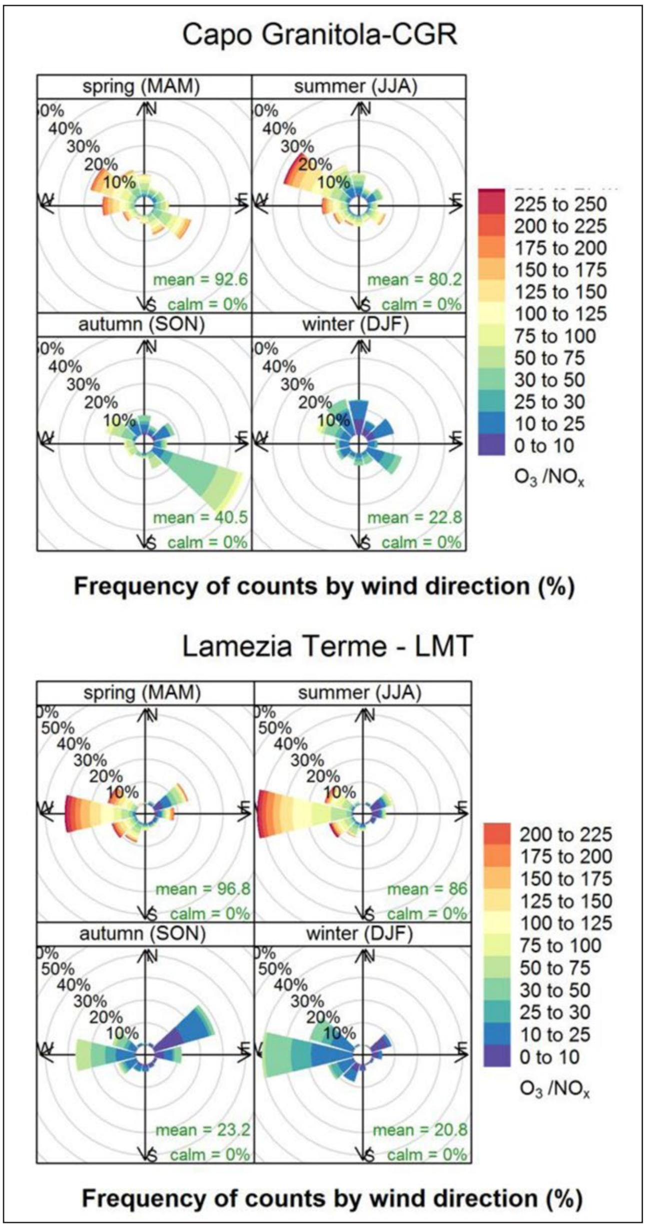

Figure 7: Analysis of seasonal O_3/NO_x ratio for CGR (up) and LMT (bottom) as a function of wind direction. O_3/NO_x ratio as a function of wind direction at CGR and LMT, showed that "fresh" combustion emissions were mostly observed when air-masses come from the land interior, while "background" conditions mostly occurred when air-masses are flowing from the sea. DOI: https://doi.org/10.1525/elementa.216.f7

Steinbacher et al., 2007), we performed a sensitivity test by halving the original NO_2 values for remote and background regimes, i.e. we re-calculated the hourly O_3/NO_x averaged ratios by applying the following formula:

$$O_3/NO_X^{text} = O_3/(NO + NO_2/2)$$

Where NO_x^{test} represents the re-calculated NO_x values for the sensitivity test, O_3, NO and NO_2 represent the measured hourly average values. In that case, the fraction of observations that can be tagged to background regime increased considerably (up to 71% at both measurement sites), while observations tagged to remote sources almost disappeared. Since, we noted statistically significant differences for the atmospheric compounds as a function of the regime classification based on the original NO_2 reading, and argued that is rather unlikely that no far-outflow conditions affected the measurement sites, we decided to retain the original NO_2 mixing ratios for RG variability discussion. The analysis of trace gases as a function of photochemical processing pointed out that all the atmospheric compounds except O_3 and SO_2 (which are maximized for nearby sources) showed decreasing values shifting from LOC to BKG with statistically significant (at the 95% confidence level) differences among the four regimes (**Table 1**). At LMT, the fresh pollution regime ($O_3/NO_x < 10$) is characterized by enhanced CH_4 values (> 2000 ppb), indicating local sources of CH_4 (possibly small but widely dispersed farms with livestock). On the other hand, it is noteworthy that CH_4 showed statistically significant higher values at CGR than at LMT for background conditions (**Table 1**).

Table 1: Average mean value ± 95% confidence level (expressed as ppb) for O_3, NO, NO_2, CO, CH_4 and SO_2 as a function of different photochemical processing: local sources (LOC), nearby sources (N-SRC), remote sources (R-SRC) and background (BKG). For CGR, data in brackets indicate values when the influence of local biogenic emissions of SO_2 and CH_4 from algae are excluded. DOI: https://doi.org/10.1525/elementa.216.t1

	CGR (ppb)			
	LOC	**N-SRC**	**R-SRC**	**BKG**
O_3	23.2 ± 0.7	37.7 ± 0.4	47.2 ± 0.4	51.5 ± 0.3
NO	0.08 ± 0.03	0.07 ± 0.01	0.04 ± 0.01	0.02 ± 0.01
NO_2	3.31 ± 0.18	1.37 ± 0.03	0.69 ± 0.01	0.37 ± 0.01
CO	168.3 ± 6.2	137.7 ± 1.2	125.9 ± 1.2	122.2 ± 0.8
CH_4	1941.4 ± 6.6 (1930.1 ± 4.3)	1933.7 ± 1.8 (1916.4 ± 1.6)	1918.5 ± 2.0 (1905.2 ± 1.8)	1908.9 ± 1.4 (1900.9 ± 1.3)
SO_2	0.07 ± 0.10 (0.03 ± 0.02)	0.10 ± 0.01 (0.07 ± 0.01)	0.11 ± 0.01 (0.10 ± 0.01)	0.05 ± 0.01 (0.05 ± 0.01)

	LMT (ppb)			
	LOC	**N-SRC**	**R-SRC**	**BKG**
O_3	25.4 ± 0.6	43.5 ± 0.4	52.0 ± 0.7	55.6 ± 0.4
NO	1.01 ± 0.13	0.22 ± 0.01	0.08 ± 0.01	0.03 ± 0.01
NO_2	5.80 ± 0.21	1.79 ± 0.03	0.67 ± 0.01	0.31 ± 0.01
CO	165.1 ± 3.8	130.0 ± 1.2	122.0 ± 1.4	118.3 ± 0.7
CH_4	2019.5 ± 7.4	1931.2 ± 2.1	1902.1 ± 2.2	1899.7 ± 1.2

3.5 Possible influence of marine biomass as source of CH_4 at CGR?

As shown in the previous Section, at CGR background CH_4 values (as deduced by O_3/NO_x analysis) were characterized by higher values in respect to LMT. With the aim of better attribute this difference, we analysed hourly CH_4 time series at CGR. We found out that enhanced CH_4 values were often associated with periods with hourly standard deviation higher than 10 ppb, indicating a high CH_4 short-term variability and the possible influence of nearby emission sources. The wind direction was from SE or NW during these events, i.e. from two small bays located at about ~100 m from the observatory along the coastline where algae and other marine biomass systematically accumulate (see Figure S3). Thus, we suspect that these events characterized by enhanced CH_4 values and variability (see supplementary material for a descriptive example) could be related to emissions from the marine algae or other biomasses along the coastline (Gurung et al., 2012). Indeed, as recently suggested by Lenhart et al. (2015), marine algae represent a CH_4 source under oxic conditions, and algae living in marine and freshwater environments might contribute to the regional and temporal oversaturation of surface waters, leading to a net exchange of CH_4 from water to atmosphere. In particular, to provide a noteworthy CH_4 production, precursors (like dimethylsulfoniopropionate DMSP, dimethyl sulfoxide, DMSO, dimethyl sulfide DMS) must either be available in high abundance or be continually synthesized.

To provide an indirect proof of the accumulated algae as a local CH_4 source, we recalculated the average values of reactive gases at CGR by excluding the events with enhanced CH_4 variability: statistically significant differences were found only for CH_4 and SO_2 (**Table 1**), stressing the possible role of algae accumulating along the coastline in influencing the variability of these atmospheric compounds through emissions of sulfide-containing precursors. Interestingly, by neglecting local events related to possible emissions from algae, we found that CH_4 BKG values at CGR and LMT were almost identical, thus indicating that air masses well representative of the large-scale background conditions are observed at both measurement sites under high O_3/NO_x conditions.

3.6 Analysis of surface ozone in the central Mediterranean PBL

The central Mediterranean basin represents a hot-spot for surface O_3 and the transport of polluted air-masses from continental Europe can be an important contribution to the occurrence of high O_3 levels over the basin. To investigate the possible impact of air mass transport from South Italy/Sicily on the surface O_3 variability in the central Mediterranean basin, we compared observations carried out at CGR with concurrent observations at the Lampedusa GAW/WMO Regional Station (LMP) which have been carried out from February to October 2015 (at this date the O_3 analyzer was sent to CGR for calibration against the I-AMICA travelling standard). The comparison against the I-AMICA TC assured the intercomparability of O_3 measurements between LMP and CGR. Both the LMP and CGR

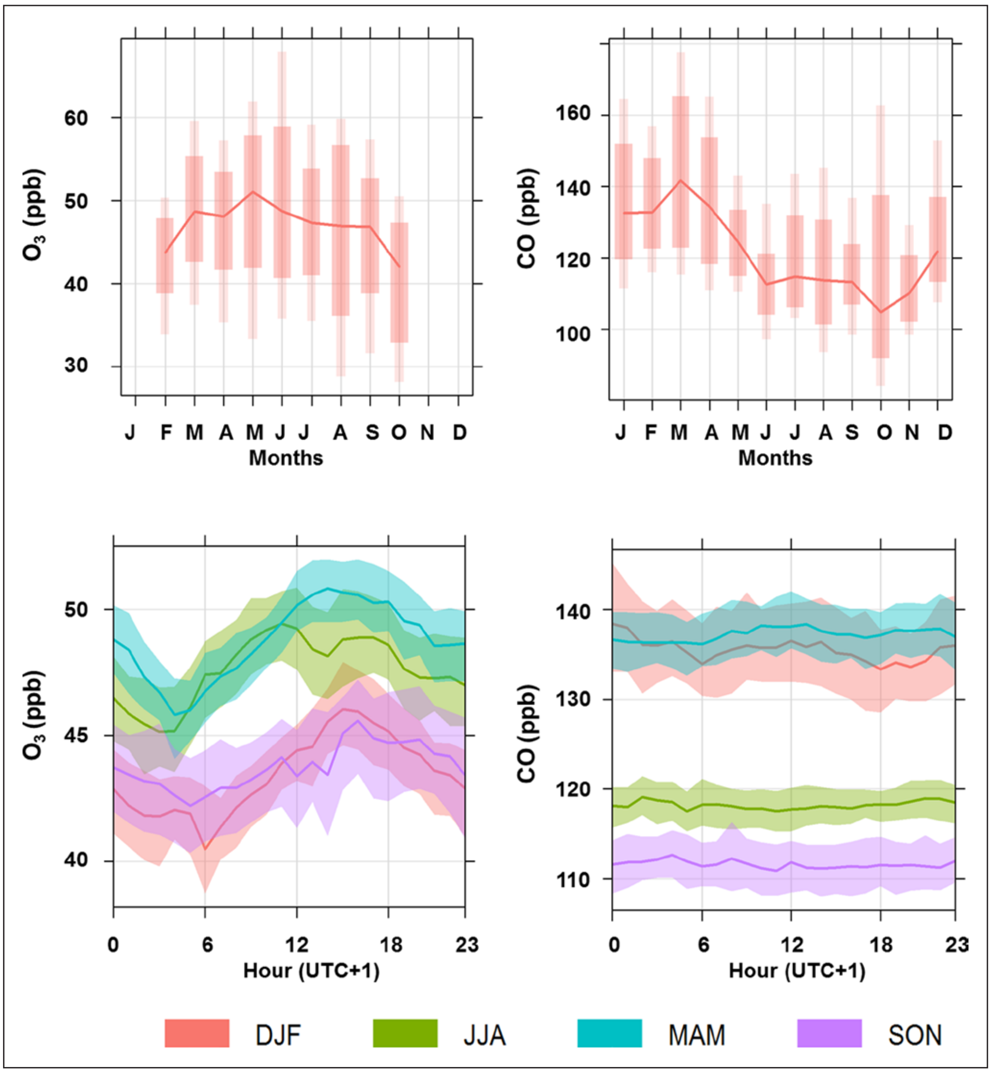

Figure 8: O_3 and CO variability at LMP. Upper plate: monthly medians (continuous line) and percentiles (10th, 25th, 75th and 90th) for hourly values of O_3 and CO at LMP. Bottom plates: seasonal average diurnal variations for O_3 and CO at LMP. The dashed areas represent the 95% confidence interval. DOI: https://doi.org/10.1525/elementa.216.f8

analyzers were evaluated against the I-AMICA TC over 21 different concentration levels ranging from 0 to 100 ppb following the methodology presented in Klausen et al. (2003). Expanded uncertainty (with coverage factor k=2) ranged from 0.75 ppb to 1.06 ppb for both the analyzers in the range 0–100 ppb. Consequently (in agreement with Boylan et al., 2005), differences between the two data sets need to be on the order of ≥ 2 ppb to be considered significant. Throughout the measurement period, LMP reported higher O_3 average value (47.2 ± 1.8 ppb) compared to CGR (40.9 ± 1.3 ppb).

On a monthly basis (**Figure 8**), at LMP, O_3 showed the highest values in late spring/early summer (i.e. May – June with 75th percentiles exceeding 55 ppb), while the lowest values were reported for October (25th percentiles lower than 35 ppb). The monthly mean average values peaked in May (50.0 ± 0.6 ppb) and then decreased towards October (40.1 ± 0.6 ppb). In respect to CGR, this seasonal cycle is more similar to what reported for background/rural sites and other observation sites in the marine boundary layer-MBL (Boylan et al., 2015; Oltmans and Levy, 1992, 1994; Tarasova et al., 2007), which are characterized by O_3 maxima during winter–spring. LMP is characterized by a smoother diurnal cycle with respect to CGR (statistically significant average diurnal variations were observed only during the winter), thus pointing out a lower influence of local processes (NO titration, photochemistry and PBL dynamics). The average diurnal deviation is about 4–5 ppb throughout the year, except in April and May when the average diurnal amplitudes reached 6–7 ppb. Average diurnal cycles were characterized by minima during night/early morning and maxima during midday/afternoon caused by a combination of low local emissions and limited boundary layer mixing.

To better understand the O_3 variability at LMP and better investigate the possible transport of air-mass rich in photochemically-produced O_3 from Sicily/southern Italy, we also considered CO time series observed at the LMP observatory. CO at LMP is measured by CRDS (Picarro G2401). The measurements are referred to CO standards provided by the Max Planck Institute for Biogeochemistry GasLab; secondary standards are used every 3 to 4 weeks, and a working standard is measured every 6 hours. The air is dried in a deep freezer at about –60°C to reduce water vapor influence. As discussed by Zellweger et al. (2012), CRDS measurements are well within the GAW data quality objectives for CO of ±2 ppb (WMO, 2010) for averaging intervals longer than 10 minutes. Hourly data are used in this study. On a monthly basis, hourly CO values showed high values during winter-spring, minima during summer and increasing values in autumn. On average, no diurnal cycles were observed for the different seasons, further stressing the lack of important combustion source at this site. Thus, since anthropogenic pollutant emissions at LMP are expected to be limited, it is conceivable that O_3 precursors within the continental outflows could contribute to the observed photochemical O_3 production. To preliminary investigate this possibility, we analyzed the HYSPLIT back-trajectory ensembles calculated for LMP, by selecting the period for which back-trajectories were travelling over the sea, passing within a 1° × 1° box centered around CGR (see Figure S4).

Then, we calculated the difference (ΔO_3 and ΔCO, respectively) between the hourly O_3 and CO at LMP and that measured at CGR at the trajectory passage. In total, 15 days from February to October 2015 (when O_3 observations were available at LMP) were selected as likely influenced by direct transport of air-masses from CGR to LMP. Almost the totality of these days (13/15) were occurring during summer. It should be noted that the relatively low number of selected days was due to the very strict criteria adopted for the air-mass selection, aimed at minimizing any contact of air masses with land surface during the transport from CGR to LMP. As deduced by back-trajectories analysis, the air-mass travel time spanned from 7 hour to 96 hour (average value: 62 hour). As shown by the histogram of the frequency distribution (Figure S5), two classes of travel time characterized the air mass transport from CGR to LMP: a "fast" transport (about 20 hour) and a "slow" transport (above 90 hours). As reported by Stohl et al. (1998), position errors of 20% of the travel distance can be considered as typical for back-trajectory calculation. For what concerns our study an average travel distance of roughly 250 km was calculated for the "fast" transport episodes, which implies a typical position error of about 50 km. For the "slow" transport episodes, the calculated travel distance was about 600 km, with a typical position error of about 120 km. Thus, the results for this transport regime must be taken with caution. To investigate O_3 dynamic as a function of travel time of air masses from CGR to LMP, we aggregated hourly ΔO_3 and ΔCO as a function of their travel time (**Figure 9**). The former selection was characterized by a significant O_3 increase at LMP with respect to CGR (ΔO_3: 6.8 ± 5.0 ppb), implying photochemical O_3 production during the transport. In general, for the "fast" transport, the ΔO_3 population was characterized by a shift towards higher values with respect to observations tagged as "slow" transport, for which ΔO_3 was not statistically different from zero. Even if possible errors in the back-trajectory calculation cannot be neglected for this classes of transport regime, this roughly indicates that the longer the air-masses remain within the Mediterranean MBL, the lower is the ΔO_3 at LMP. Even if the effect of mixing and dilution for longer travel time can play a not negligible role, albeit difficult to quantify, this would suggest that the summer MBL represents a net O_3 sink. By calculating the ΔO_3 difference between the two transport regimes, an average O_3 loss rate of about 3.0 ppb/day is obtained considering the median transport time (33 and 96 hours) as representative for the two regimes. In particular, the following formula was used to calculate the O_3 loss rate:

$$O_3^{lossate} = \left(\Delta O_3^{slow} - \Delta O_3^{fast}\right)\left(t^{slow} - t^{fast}\right)$$

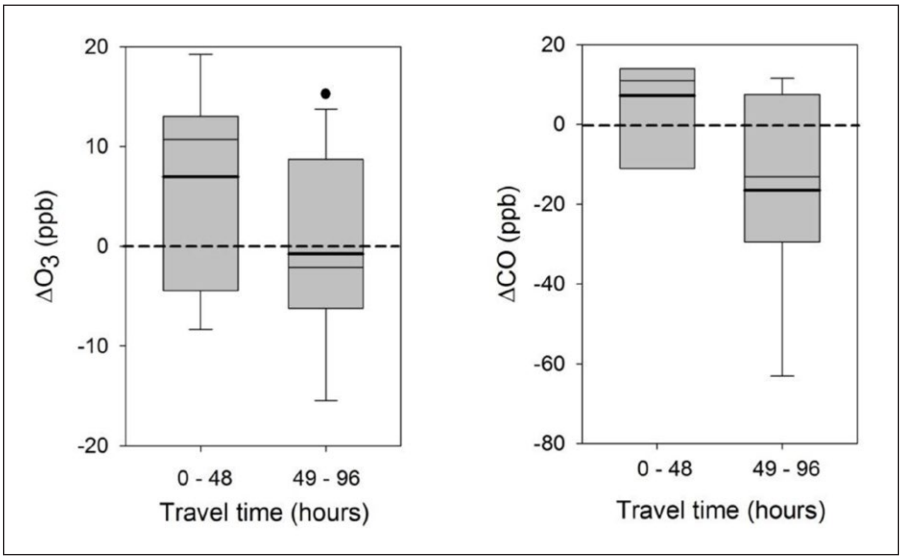

Figure 9: ΔO_3 and ΔCO values as a function of the two different classes of travel time for air-masses from CGR to LMP. The boxes and whiskers denote the 10th, 25th, 50th, 75th and 90th percentiles of ΔO_3 and ΔCO as a function of the two different classes of travel time for air-masses from CGR to LMP. The tick lines represent the mean average values. DOI: https://doi.org/10.1525/elementa.216.f9

Where t^{slow} (t^{fast}) is the median value of transport time for the "slow" ("fast") transport regime.

Concerning CO, the average ΔCO was not statistically different from zero for the "fast" transport (i.e. very similar CO values were observed at CGR and at LMP) but it was lower than zero (significant at the 95% confidence level) for the "slow" transport, indicating CO "loss" during the transport from CGR to LMP. This can be explained considering the occurrence of different processes (e.g. OH removal within marine PBL or air-mass dilution along the transport).

4. Conclusions

This work presents a preliminary characterization of relevant trace gases (O_3, NO, NO_2, CO, CH_4, SO_2) in the central Mediterranean basin, analyzing in situ measurements at three new permanent observatories in Southern Italy, set up in the framework of the I-AMICA Project. Several years of data should be analyzed to provide a robust and conclusive characterization of these trace gases at the considered observatories. Nevertheless, since virtually no data about RGs and CH_4 are available in the framework of WMO/GAW in the South Italy, this work would represent a notable contribution towards a more accurate knowledge of tropospheric chemistry in the central Mediterranean region. These new GAW regional stations are representative of different environmental and atmospheric conditions. As deduced from the analysis of trace gas average values and variability among the three measurement sites, CGR appeared to be the location most representative of background conditions, with a limited impact of local/regional emissions under land breeze circulation. ECO, representative of the Lecce suburban area, is the site most affected by direct emissions of anthropogenic pollutants. An intermediate situation was found at LMT, where polluted conditions affected the measurements with easterly (land) breeze (bringing emissions from the interior of the region), and observations were well representative of the regional background under a westerly (sea) breeze circulation.

At all the measurement sites a well-defined diurnal cycle affected RG variability due to a combination of sea/land breeze system (especially at CGR and LMT), PBL dynamics, local/regional emissions, and photochemistry. In particular, for the different RG here considered, the differences among the three station were minimized during day-time, supporting the picture that when marine air-masses affected CGR and LMT coastal sites and well developed mixed PBL affected ECO, the observations are well representative of the regional background of the Mediterranean basin. An impact of anthropogenic emissions probably related with touristic activity, is evident at LMT (and somewhat at CGR in summer, as traced by the higher NO_x peak in the early morning). An evident daytime SO_2 peak was observed at CGR during winter, which was tentatively related to the impact of marine biogenic and/or anthropogenic ship emissions. A definitive attribution of the high SO_2 values (well above the instrumental detection limit) observed during winter daytime to DMS oxidation or to anthropogenic ship emissions is challenging.

For LMT and CGR, where reliable NO_x measurements were available during the investigation period, we calculated O_3/NO_x ratios to characterize the degree of photochemical process of sampled air masses. Our O_3/NO_x estimate can be affected by uncertainties related to a not optimal frequency of NO_x calibration, use of Mo-converter and no corrections of O_3 and water vapor interferences on NO_x measurements. To analyze the effect of this weakness a sensitivity study has been carried out by varying the observed NO_2 values. The obtained results suggested that the presented results were reasonably robust. Nevertheless, further implementation of the instrumental and calibration set-up (i.e. implementation of high-frequency calibration and use of photolytic converter) is foreseen at these new measurement sites. According to O_3/NO_x variability, local emissions appeared to influence CGR and LMT in 4.0% and 20% of the hourly data, nearby sources conditions in 39% and 40%, remote sources in 31% and 14%, while background O_3/NO_x were observed in 26% of cases for both the measurement sites. At both measurement sites, most of the background O_3/NO_x were observed during daytime, when air masses from offshore usually affected the measurement sites. It is noteworthy that under background conditions, significantly different CH_4 values were observed at CGR and LMT indicating the presence of local sources. We suggested that these differences can be attributed to biogenic (oxic) emissions from algae or other biomasses accumulated along the coastline, while emissions from live stocks possibly lead the occurrence of CH_4 peaks at LMT. Again, in the future, when a longer measurement period will be available these processes will be further investigated also to investigate their interannual variability.

Finally, we compared the O_3 and CO observations carried out at CGR and LMP (a GAW/WMO observatory located on Lampedusa Island) to provide first hints on the outflow from Southern Italy to the Mediterranean Sea. For the observed "outflow" events, we found that O_3 at LMP was significantly higher (+6.8 ppb, on average) than at CGR for travel time lower than 48 h. The obtained value is larger than the expanded uncertainty which characterized the two O_3 analyzers working at LMP and CGR. This would imply the occurrence of efficient photochemical production within the air-masses flowing from CGR to LMP. This increases could not be detected for air-masses with calculated travel time longer than 48 h. Even if other processes should be considered (e.g. air-mass mixing and dilution along transport, different meteorological conditions leading to this different transport regime) and relatively large uncertainty is expected to affect the back-trajectory calculation for this regime, this would suggest that the central Mediterranean MBL represents a O_3 sink, especially in summer for air-masses with age roughly higher than 48 h, with a typical O_3 reduction of about 3.0 ppb/day. In the future, the extension of the analyses here presented by using a longer data-set will provide the opportunity to investigate interannual variability and to provide a more robust assessment of the preliminary results presented in this work.

Data accessibility statement

CGR CO and CH_4 data were available at the GAW Word Data Center for Greenhouse Gases (WDCGG, http://ds.data.jma.go.jp/gmd/wdcgg/cgi-bin/wdcgg/access-data.cgi?cntry=Italy&index=CGR637N00-ISAC&para=CO2&select=inventory). The remaining data (O_3, NO_x, SO_2 and meteorological parameters) were submitted to World Data Centre for Reactive Gases (WDCRG) hosted by NILU (Norwegian Institute for Air Research, http://ebas.nilu.no) on July 2015 but they are still not published. LMT and ECO data were submitted to WDCGG (CO, CH_4) and WDCGR (O_3, NO_x) but they are still not published.

Supplemental Files

The supplemental files for this article can be found as follows:

- **Figure S1.** Seasonal average diurnal variation of wind speed (WS), relative humidity (RH) and water vapor (H_2O) at the three I-AMICA sites. Dashed areas denote the 96% confidence levels. Time is expressed in local time (UTC+1). DOI: https://doi.org/10.1525/elementa.216.s1
- **Figure S2.** NO/NO_2 and CO/NO_x variability at CGR (left) and LMT (right). DOI: https://doi.org/10.1525/elementa.216.s2
- **Figure S3.** Satellite image (courtesy of Google Earth) of the CGR location. The two small bays with alga accumulation are reported together with CGR location (red triangle). Below a representative event with concurrent CH_4 and SO_2 enhancements under south-westerly wind (i.e. from the bay) is shown. DOI: https://doi.org/10.1525/elementa.216.s3
- **Figure S4.** Patterns of air-masses moving from CGR to LMP during the investigated period. DOI: https://doi.org/10.1525/elementa.216.s4
- **Figure S5.** Histogram of the frequency distribution of travel times for air-masses from CGR to LMP. DOI: https://doi.org/10.1525/elementa.216.s5

Acknowledgements

The authors gratefully acknowledge the NOAA Air Resources Laboratory (ARL) for the provision of the HYSPLIT transport and dispersion model and/or READY website (http://www.ready.noaa.gov) used in this publication. Some of the plots presented in this work were produced by using the "R" package "Openair" (Carslaw and Ropkins, 2012). The authors gratefully thank CNR-IAMC or hosting the CGR observatory at his own scientific campus. A special mention is due to Mr. Giovanni Ceccherillo and Dr. Domenico Spoto (CNR-IAMC) for their technical support at the CGR observatory. The standard gases for CO calibrations at Lampedusa were provided by the GasLab of the Max Planck Institute for Biogeochemistry within the Integrated non-CO_2 Gas Observing System (In-GOS) Project, supported by the European Union.

Funding information

I-AMICA Project was funded by the Italian National Operation Program "Ricerca e Competitività" (Research and Competitiveness) 2007–2013 (PON "R&C"). The paper publication and open-access costs were supported by the Project of National Interest NEXTDATA.

Competing interests

The authors have no competing interests to declare.

Author contributions

- Contributed to conception and design: <PC>
- Contributed to acquisition of data: <MB, FC, IA, DG, AD, CRC, DC, DS, TDI, SP, AM>
- Contributed to analysis and interpretation of data: <PC, MM, PB>
- Drafted and/or revised the article: <PC, CRC, DC, MM, PB>
- Approved the submitted version for publication: <PC, MB, FC, IA , DG, AD, CRC, DC, DS, TDI, SP AM, MM, PB>

References

Becagli, S, Sferlazzo, DM, Pace, G, di Sarra, A, Bommarito, C, Calzolai, G, Ghedini, C, Lucarelli, F, Meloni, D, Monteleone, F, Severi, M, Traversi, R and **Udisti, R** 2012 Evidence for heavy fuel oil combustion aerosols from chemical analyses at the island of Lampedusa: a possible large role of ships emissions in the Mediterranean. *Atmos Chem Phys* **12**: 3479–3492. DOI: https://doi.org/10.5194/acp-12-3479-2012

Boersma, KF, Jacob, DJ, Trainic, M, Rudich, Y, DeSmedt, I, Dirksen, R and **Eskes, H** 2009 Validation of urban NO_2 concentrations and their diurnal and seasonal variations observed from the SCIAMACHY and OMI sensors using in situ surface measurements in Israeli cities. *Atmos Chem Phys* **9**: 3867–3879. DOI: https://doi.org/10.5194/acp-9-3867-2009

Boylan, P, Helmig, D and **Oltmans, S** 2015 Ozone in the Atlantic Ocean marine boundary layer. *Elem Sci Anth* **3**: 000045. DOI: https://doi.org/10.12952/journal.elementa.000045

Carslaw, DC and **Ropkins, K** 2012 Openair — an R package for air quality data analysis. *Environ Model Soft* **27–28**: 52–61. DOI: https://doi.org/10.1016/j.envsoft.2011.09.008

Cesari, D, Genga, A, Ielpo, P, Siciliano, M, Mascolo, G, Grasso, FM and **Contini, D** 2014 Source apportionment of PM2.5 in the harbour–industrial area of Brindisi (Italy): Identification and estimation of the contribution of in-port ship emissions. *Sci Tot Environ* **497–498**: 392–400. DOI: https://doi.org/10.1016/j.scitotenv.2014.08.007

Chen, H, Winderlich, J, Gerbig, C, Hoefer, A, Rella, CW, Crosson, ER, Van Pelt, AD, Steinbach, J, Kolle, O, Beck, V, Saube, BC, Gottlieb, EW, Chow, VY, Santoni, GW and **Wofsy, SC** 2010 High-accuracy continuous airborne measurements of greenhouse gases (CO_2 and CH_4) using the cavity ringdown spectroscopy (CRDS) technique. *Atmos Meas Tech* **3**: 375–386. DOI: https://doi.org/10.5194/amt-3-375-2010

Contini, D, Genga, A, Cesari, D, Siciliano, M, Donateo, A, Bove, MC and **Guascito, MR** 2010 Characterisation and source apportionment of PM10 in an urban background site in Lecce. *Atmos Res* **95**: 40–54. DOI: https://doi.org/10.1016/j.atmosres.2009.07.010

Crutzen, PJ, Lawrence, MG and **Pőschl, U** 1999 On the background photochemistry of tropospheric ozone, *Tellus* **51**: 123–146. DOI: https://doi.org/10.3402/tellusb.v51i1.16264

Draxler, RR and **Hess, GD** 1998 An overview of the HYSPLIT_4 modeling system of trajectories, dispersion, and deposition. *Austral Met Mag* **47**: 295–308.

Duncan, BN, West, JJ, Yoshida, Y, Fiore, AM and **Ziemke, JR** 2008 The influence of European pollution on ozone in the Near East and northern Africa. *Atmos Chem Phys* **8**: 2267–2283. DOI: https://doi.org/10.5194/acp-8-2267-2008

EEA 2013 The impact of international shipping on European air quality and climate forcing. *Technical report 4/2013*.

Federico, S, Pasqualoni, L, Sempreviva, AM, De Leo, L, Avolio, E, Calidonna, CR and **Bellecci, C** 2010 The seasonal characteristics of the breeze circulation at a coastal Mediterranean site in South Italy. *Adv Sci Res* **4**: 47–56. DOI: https://doi.org/10.5194/asr-4-47-2010

Gilge, S, Plass-Duelmer, C, Fricke, W, Kaiser, A, Ries, L, Buchmann, B and **Steinbacher, M** 2010 Ozone, carbon monoxide and nitrogen oxides time series at four alpine GAW mountain stations in central Europe. *Atmos Chem Phys* **10**: 12295–12316. DOI: https://doi.org/10.5194/acp-10-12295-2010

Gilge, S, Plass-Duelmer, C, Roher, F, Steinbacher, M, Fjaeraa, AM, Lageler, F and **Walden, J** 2014 WP4-NA4: Trace gases networking: Volatile organic carbon and nitrogen oxides Deliverable D4.10: Standardized operating procedures (SOPs) for NO_{xy}. Version: 2014/09/19.

Giorgi, F and **Lionello, P** 2008 Climate change projections for the Mediterranean region. *Glob Planet Chang* **63**: 90–104. DOI: https://doi.org/10.1016/j.gloplacha.2007.09.005

Gurung, A, Van Ginkel, SW, Kang, W-C, Qambrani, NA, Oh, S-E 2012 Evaluation of marine biomass as a source of methane in batch tests: A lab-scale study. *Energy* **43**(1): 396–401. DOI: https://doi.org/10.1016/j.energy.2012.04.005

Henne, S, Furger, M, Nyeki, S, Steinbacher, M, Neininger, B, de Wekker, SFJ, Dommen, J, Spichtinger, N, Stohl, A and **Prévôt, ASH** 2004 Quantification of topographic venting of boundary layer air to the free troposphere, *Atmos Chem Phys* **4**: 497–509. DOI: https://doi.org/10.5194/acp-4-497-2004

Jalkanen, J-P, Johansson, L and **Kukkonen, J** 2016 A comprehensive inventory of ship traffic exhaust emissions in the European sea areas in 2011. *Atmos Chem Phys* **16**: 71–84. DOI: https://doi.org/10.5194/acp-16-71-2016

Klausen, J, Zellweger, C, Buchmann, B and **Hofer, P** 2003 Uncertainty and bias of surface ozone measurements at selected Global Atmosphere Watch sites. *J Geophys Res* **108**: 4622. DOI: https://doi.org/10.1029/2003JD003710

Kouvarakis, G and **Mihalopoulos, N** 2002 Seasonal variation of dimethylsulfide in the gas phase and of methanesulfonate and non-sea-salt sulfate in the aerosols phase in the Eastern Mediterranean atmosphere. *Atmos Environ* **36**(6): 929–938. DOI: https://doi.org/10.1016/S1352-2310(01)00511-8

Lana, A, et al. 2011 An updated climatology of surface dimethlysulfide concentrations and emission fluxes in the global ocean. *Glob Biogeochem Cyc* **25**: GB1004. DOI: https://doi.org/10.1029/2010GB003850

Lelieveld, J, Berresheim, H, Borrmann, S, Crutzen, PJ, Dentener, FJ, Fischer, H, Feichter, J, Flatau, PJ, Heland, J, Holzinger, R, Korrmann, R, Lawrence, MG, Levin, Z, Markowicz, KM, Mihalopoulos, N, Minikin, A, Ramanathan, V, Reus, MD, Roelofs, GJ, Scheeren, HA, Sciare, J, Schlager, H, Schultz, M, Siegmund, P, Steil, B, Stephanou, EG, Stier, P, Traub, M, Warneke, C, Williams, J and **Ziereis, H** 2002 Global Air Pollution Crossroads over the Mediterranean. *Science* **298**: 794–799. DOI: https://doi.org/10.1126/science.1075457

Lenhart, K, Klintzsch, T, Langer, G, Nehrke, G, Bunge, M, Schnell, S and **Keppler, F** 2015 Evidence for methane production by marine algae (Emiliana huxleyi) and its implication for the methane paradox in oxic waters. *Biogeosci Discuss* **12**: 20323–20360. DOI: https://doi.org/10.5194/bgd-12-20323-2015

Li, J, Reiffs, A, Parchatka, U and **Fischer, H** 2015 In situ measurements of atmospheric CO and its correlation with NOx and O_3 at a rural mountain site. *Metrol Meas Syst* **22**: 25–38. DOI: https://doi.org/10.1515/mms-2015-0001

Mallet, M, Dubovik, O, Nabat, P, Dulac, F, Kahn, R, Sciare, J, Paronis, D and **Léon, JF** 2013 Absorption properties of Mediterranean aerosols obtained from multi-year ground-based remote sensing observations. *Atmos Chem Phys* **13**: 9195–9210. DOI: https://doi.org/10.5194/acp-13-9195-2013

Mangia, C, Martano, P, Miglietta, MM, Morabito, A and **Tanzarella, A** 2004 Modelling local winds over the Salento peninsula. *Meteoro Appl* **11**: 231–244. DOI: https://doi.org/10.1017/S135048270400132X

Martins, DK, Stauffer, RM, Thompson, AM, Knepp, TN and **Pippin, N**. 2012 Surface ozone at a coastal suburban site in 2009 and 2010: Relationship to chemical and meteorological processes. *J Geophys Res* **117**(D05): 306. DOI: https://doi.org/10.1029/2011JD016828

Monks, PS, et al. 2009 Atmospheric composition change – global and regional air quality. *Atmos.*

Environ. **43**(33): 5268–5350. DOI: https://doi.org/10.1016/j.atmosenv.2009.08.021

Morgan, WT, Allan, JD, Bower, KN, Highwood, EJ, Liu, D, McMeeking, GR, Northway, MJ, Williams, PI, Krejci, R and **Coe, H** 2010 Airborne measurements of the spatial distribution of aerosol chemical composition across Europe and evolution of the organic fraction. *Atmos Chem Phys* **10**: 4065–4083. DOI: https://doi.org/10.5194/acp-10-4065-2010

Novelli, PC, Masarie, KA, Lang, PM, Hall, BD, Myers, RC and **Elkins, JW** 2003 Re-analysis of tropospheric CO trends: Effects of the 1997–1998 wild fire., *J Geophys Res* **108**: 4464. DOI: https://doi.org/10.1029/2002JD003031

Oltmans, SJ and **Levy, HI** 1992 Seasonal cycle of surface ozone over the western North Atlantic. *Nature* **358**: 392–394. DOI: https://doi.org/10.1038/358392a0

Oltmans, SJ and **Levy, HI** 1994 Surface ozone measurements from a global network. *Atmos. Environ.* **28**: 9–24. DOI: https://doi.org/10.1016/1352-2310(94)90019-1

Parrish, DD, Allen, DT, Bates, TS, Estes, M, Fehsenfeld, FC, Feingold, G, Ferrare, R, Hardesty, RM, Meagher, JF, Nielsen-Gammon, JW, Pierce, RB, Ryerson, TB, Seinfeld, JH and **Williams, EJ** 2009 Overview of the Second Texas Air Quality Study (TexAQS II) and the Gulf of Mexico Atmospheric Composition and Climate Study (GoMACCS). *J Geophys Res* **114**(D00): F13. DOI: https://doi.org/10.1029/2009JD011842

Querol, X, Alastuey, A, Pey, J, Cusack, M, Pérez, N, et al. 2009 Variability in regional background aerosols within the Mediterranean. *Atmos Chem Phys* **9**: 4575–4591. DOI: https://doi.org/10.5194/acp-9-4575-2009

Ramanathan, V and **Xu, Y** 2010 The Copenhagen Accord for limiting global warming: Criteria, constraints, and available avenues. *PNAS* **107**(18): 8055–8062. DOI: https://doi.org/10.1073/pnas.1002293107

Rella, CW, Chen, H, Andrews, AE, Filges, A, Gerbig, C, Hatakka, J, Karion, A, Miles, NL, Richardson, SJ, Steinbacher, M, Sweeney, C, Wastine, B and **Zellweger, C** 2013 High accuracy measurements of dry mole fractions of carbon dioxide and methane in humid air. *Atmos Meas Tech* **6**: 837–860. DOI: https://doi.org/10.5194/amt-6-837-2013

Ricaud, P, Sič, B, El Amraoui, L, Attié, J-L, Zbinden, R, Huszar, P, Szopa, S, Parmentier, J, Jaidan, N, Michou, M, Abida, R, Carminati, F, Hauglustaine, D, August, T, Warner, J, Imasu, R, Saitoh, N and **Peuch, V-H** Impact of the Asian monsoon anticyclone on the variability of mid-to-upper tropospheric methane above the Mediterranean Basin. *Atmos Chem Phys.* **14**: 11427–11446. DOI: https://doi.org/10.5194/acp-14-11427-2014

Safieddine, S, Boynard, A, Coheur, P-F, Hurtmans, D, Pfister, G, Quennehen, B, Thomas, JL, Raut, J-C, Law, KS, Klimont, Z, Hadji-Lazaro, J, George, M, and **Clerbaux, C** 2014 Summertime tropospheric ozone assessment over the Mediterranean region using the thermal infrared IASI/MetOp sounder and the WRF-Chem model *Atmos Chem Phys* **14**: 10119–10131. DOI: https://doi.org/10.5194/acp-14-10119-2014

Saliba, M, Ellul, R, Camilleri, L and **Güsten, H** 2008 A 10-year study of background surface ozone concentrations on the island of Gozo in the Central Mediterranean. *J Atmos Chem* **60**: 117–135, 2008. DOI: https://doi.org/10.1007/s10874-008-9112-3

Schultz, MG, Akimoto, H, Bottenheim, J, Buchmann, B, Galbally, IE, et al. 2015 The Global Atmosphere Watch reactive gases measurement network. *Elem Sci Anth* **3**: 000067. DOI: https://doi.org/10.12952/journal.elementa.000067

Seinfeld, JH and **Pandis, SN** 1998 Atmospheric chemistry and physics: from air pollution to climate change. *Wiley Interscience*, 1326 pp., New York, USA.

Shindell, D, et al. 2012 Simultaneously Mitigating Near-Term Climate Change and Improving Human Health and Food Security. *Science* **335**: 183–189. DOI: https://doi.org/10.1126/science.1210026

Stein, AF, Draxler, RR, Rolph, GD, Stunder, BJB, Cohen, MD and **Ngan, F** 2015 NOAA's HYSPLIT atmospheric transport and dispersion modeling system. *Bull. Amer Meteor Soc* **96**: 2059–2077. DOI: https://doi.org/10.1175/BAMS-D-14-00110.1

Steinbacher, M, Zellweger, C, Schwarzenbach, B, Bugmann, S, Buchmann, B, Ordóñez, C, Prevot, ASH and **Hueglin, C** 2007 Nitrogen oxide measurements at rural sites in Switzerland: Bias of conventional measurement techniques. *J Geophys Res* **112**(D11): 307. DOI: https://doi.org/10.1029/2006JD007971

Stohl, A 1998 Computation, accuracy and applications of trajectories – a review and bibliography. *Atmos Environ* **32**: 947–996. DOI: https://doi.org/10.1016/S1352-2310(97)00457-3

Tarasova, OA, Brenninkmeijer, CAM, Jöckel, P, Zvyagintsev, AM and **Kuznetsov, GI** 2007 A climatology of surface ozone in the extra tropics: cluster analysis of observations and model results. *Atmos Chem Phys* **7**: 6099–6117. DOI: https://doi.org/10.5194/acp-7-6099-2007

Turquety, S, Menut, L, Bessagnet, B, Anav, A, Viovy, N, Maignan, F and **Wooster, M** 2014 APIFLAME v1.0: high-resolution fire emission model and application to the Euro-Mediterranean region. *Geos Mod Dev* **7**: 587–612. DOI: https://doi.org/10.5194/gmd-7-587-2014

UNEP and **WMO** 2011 Integrated Assessment of Black Carbon and Tropospheric Ozone. UNEP, Nairobi.

Vautard, R, Honoré, C, Beekmann, M and **Rouil, L** 2005 Simulation of ozone during the August 2003 heat wave and emission control scenarios. *Atmos Environ* **39**: 2957–2967.

Volz-Thomas, A, Beekmann, M, Derwent, D, Law, K, Lindskog, A, Prevot, A, Roemer, M, Schultz, M, Schurath, U, Solberg, S and **Stohl, A** 2002 Tropospheric Ozone and its Control, in: Towards Cleaner Air for Europe – Science, Tools and Applications. Part 1: Results from the EUROTRAC-2; Synthesis and Integration (S&I) Project, edited by: Builtjes, P. J.-H., Harrison, R. M., Midgley, P. M., and Tørsen, K., International Scientific Secretariat, Munchen, Germany, 73–122.

WMO 2010 Guidelines for the Measurement of Atmospheric Carbon Monoxide, GAW Report No. 192, World Meteorological Organization, Geneva, Switzerland.

Yang, M, Bell, TG, Hopkins, FE and **Smyth, TJ** 2016 Attribution of Atmospheric Sulfur Dioxide over the English Channel to Dimethylsulfide and Changing Ship Emissions. *Atmos Chem Phys Discuss* in review, 2016. DOI: https://doi.org/10.5194/acp-2016-56

Zellweger, C, Steinbacher, M and **Buchmann, B** 2012 Evaluation of new laser spectrometer techniques for in-situ carbon monoxide measurements. *Atmos Meas Tech* **5**: 2555–2567. DOI: https://doi.org/10.5194/amt-5-2555-2012

How to cite this article: Cristofanelli, P, Busetto, M, Calzolari, F, Ammoscato, I, Gullì, D, Dinoi, A, Calidonna, C R, Contini, D, Sferlazzo, D, Di Iorio, T, Piacentino, S, Marinoni, A, Maione, M and Bonasoni, P 2017 Investigation of reactive gases and methane variability in the coastal boundary layer of the central Mediterranean basin. *Elem Sci Anth,* 5: 12, DOI: https://doi.org/10.1525/elementa.216

Domain Editor-in-Chief: Detlev Helmig, University of Colorado Boulder

Guest Editor: Frank Flocke, National Center for Atmospheric Research

Part of an *Elementa* Special Feature: Reactive Gases in the Global Atmosphere

Submitted: 24 June 2016 **Accepted:** 17 January 2017 **Published:** 27 March 2017